JOINT EUROPEAN TORUS

JET–P(88)58

P.H. Rebut
and P.P. Lallia

JET Results and the Prospects for Fusion

JET Results and the Prospects for Fusion

P.H. Rebut
and P.P. Lallia

JET-Joint Undertaking, Culham Science Centre, OX14 3DB, Abingdon, UK

Preprint of an Invited Paper presented at the 15th Symposium on Fusion Technology,
Utrecht, The Netherlands, 19th September – 23rd September 1988

15th November 1988

15TH SYMPOSIUM ON FUSION TECHNOLOGY, UTRECHT, THE NETHERLANDS,

19TH-23RD SEPTEMBER 1988

JET RESULTS AND THE PROSPECTS FOR FUSION

P.H. Rebut and P.P. Lallia

JET Joint Undertaking, Abingdon, Oxon, OX14 3EA, U.K.

ABSTRACT

Recent experiments on JET with increased additional power have resulted in plasma parameters close to those of a thermonuclear reactor. Electron and ion temperature significantly in excess of 10keV have been simultaneously achieved at a plasma density of $2 \times 10^{19} m^{-3}$; transiently, during an H-mode the fusion product $(\hat{n}_i \hat{T}_i \tau_E)$ has reached $3 \times 10^{20} m^{-3}.keV.s$ at temperatures exceeding 5keV; and plasma current up to 7MA (for 2s) have been achieved. However, degradation of confinement with increased power is observed in all regimes.

The major heat and particle transport phenomena observed in Tokamaks can be interpreted as resulting from a magnetic turbulence, in some respects analogous to the turbulence existing in fluids when the fluid velocity exceeds a certain threshold value. This interpretation has led to local

transport and global scaling laws giving satisfactory agreement with experimental results. Accordingly, the fusion product would scale as $I^2B_t R^{1/2}$ for a fixed Troyon factor. Reaching ignition would require a plasma current close to 30MA at a moderate field value of 4.5T.

To fully tackle the problems of a controlled burning plasma for at least days in semi-continuous operation, the plasma of the next step tokamak should be similar in size and performance to an energy producing reactor. The scientific and technical aims of such a machine should be to study a burning plasma, to test wall technology, to provide a test-bed for breeding blankets and above all to demonstrate the potential and viability of fusion as an energy source.

The main characteristics of the design of a thermonuclear furnace dedicated to these objectives are presented. Basically the plasma parameters are scaled up from JET by a linear factor of 2.5. Magnets, either superconducting or of copper, should be able to operate continuously. The present design uses watercooled copper magnets to benefit from proven technology and consists of 20 identical sectors. Each incorporates a toroidal field coil, mechanical structure and a part of the vacuum vessel wall as one integrated unit. A single-null divertor configuration ensures helium exhaust and possibly benefits from an H-mode to reach the ignition domain. The X-point position relative to the dump plates would be swept to limit the wall loading to $2MW/m^2$. By changing the operating density, the thermonuclear power could be varied from 0.5 to 4GW(th), according to requirements on power loading and tritium consumption.

I INTRODUCTION

JET is now about mid-way through its experimental programme and its achievements can be usefully compared to the Project objectives, which are:

1. The scaling of plasma behaviour as parameters approach the reactor range;
2. The plasma-wall interaction in these conditions:
3. The study of plasma heating;
4. The study of α-particle production, confinement and consequent plasma heating.

At this stage, the first three aspects have been extensively addressed and a general pattern of the plasma behaviour has emerged. Consequently, it is possible to draw some conclusions relating to the requirements and parameters of a next device.

The present paper is structured as follows. Section II summarizes the major results obtained on JET with their direct implications for a future thermonuclear reactor. In particular, a distinction is made between the achievements which can safely be regarded as steady-state (i.e. fully reactor relevant), and those corresponding to a more transient state of the plasma. Section III briefly describes a possible interpretation of the transport phenomena prevailing in a tokamak and its corresponding scaling. The performance of several 'next-step' devices are also calculated using a simplified 1-D transport code. General considerations governing the choice of a "next step tokamak" are presented in section IV. In section V, a specific "thermonuclear furnace", JIT, is proposed as a desirable step towards a prototype demonstration fusion reactor.

II MAJOR JET RESULTS AND CONSEQUENCES FOR A REACTOR

II.1 Achievements

The technical features of JET and the latest experimental results have been detailed elsewhere [1,2]. A number of major enhancements were carried out during the 1987 shut-down and are listed in Table 1. Fig.1 shows the status inside the vacuum vessel at the beginning of the 1988 operational period (which is due to end in September). New features have extended the operational domain and, in particular, have permitted the following technical and scientific achievements.

1. In quasi steady-state:

- plasma current, I_p, of 7MA has been obtained for 2s;
- JET has operated routinely with I_p above 5MA and a current of 6MA has been maintained for 7s;
- ion and electron temperatures T_i and T_e, in excess of 5keV have been sustained for over 20s at a plasma current of 3MA (see Fig.2);
- additional power up to 24MW has been delivered to a 5MA plasma producing a total energy stored of 8.8MJ (see Fig.3);

- both electron and ion temperatures simultaneously in excess of 10keV for 2s were observed at a plasma density of $2\times10^{19}m^{-3}$ (see Fig.4).

2. In a transient situation (where density, temperature or internal inductance were still varying)

- routine operation with a magnetic separatrix at I_p=4.5MA. H-mode plasmas were regularly observed during neutral beam heating. A record H-mode at 5MA has been obtained. Transiently, during an H-mode, the fusion product $(\hat{n}_i \cdot \hat{T}_i \cdot \tau_E)$ has reached $3x10^{20}m^{-3}.keV.s$ at temperatures exceeding 5keV (see Fig.5);
- the total plasma energy content has exceeded 10MJ during an H-mode;
- the maximum neutron yield has reached $9x10^{15}n/s$ produced by deuterium-deuterium fusion reactions during an H-mode at 4.5MA; the plasma was heated by 12MW of deuterium beams at an energy of 80keV;
- high peaked density plasmas were obtained by using pellet injection ($n_{eo}>10^{20}m^{-3}$). Consecutive on-axis ICRF heating of such target plasmas produced transiently peak electron pressures in excess of 1 bar.
- "monster" sawteeth are seen with ICRH (minority heating) during which q_0, the safety factor at the centre, decrease below 1 (0.8) (see Fig.3).

Consequences for a Reactor

Plasmas of thermonuclear quality have been produced in JET and no adverse effects have been observed when both electron and ion temperatures reached thermonuclear reactor values. However, the record values of neutron yield, pressure and total energy have been obtained while the plasma was in a non-steady-state situation. It seems wise to extrapolate the performance of a future machine by starting from discharges already obtained and truly stationary. Transient improvements may prove to be useful to overcome the ignition pass but should not be relied upon when working

quasi-continuously at full fusion power required routinely in a reactor.

II.2 Energy Confinement and the Fusion Product

Degradation of energy confinement with additional power is now a well known phenomenon. Recent experiments on JET have extended such observations to higher input power. Fig.6 shows the measured energy confinement time as a function of total power in JET for limiter and L-mode discharges. In this data, the time derivative of the plasma energy content does not exceed 10% of the input power. At high power, the improvement with increased current is obvious but a detailed examination of an individual scan shows a more complex pattern. The gain due to the current saturates in JET when the safety factor at the plasma boundary q_a decreases below 4, since flattening of the pressure profile results from sawtooth relaxations.

Here the safety factor q_a is defined by the current,

$$\text{i.e.} \quad q_a = \frac{2\pi abB_t}{\mu_o I_p R}. \tag{1}$$

The notation q_ψ is used when q is defined by the magnetic flux.

For the same input power but with a magnetic separatrix limiting the plasma - the so called X-point operation - the confinement of the plasma can bifurcate to a higher value, the H-mode. Fig.7 shows the energy confinement time for JET H-mode discharges. As previously,

the time derivative of the plasma energy content is small for these data, but the density is still rising while the temperature is decreasing. No significant difference was observed between single null and double null discharges. While at low power, τ_E can exceed 1s (i.e. comparable to the ohmic confinement time). It can also show a degradation with power at least as severe as in the L-mode. Similarly, confinement increases with I_p.

Consequences for a Reactor

The degradation of confinement time with the input power is considered a major threat to the success of future tokamak reactor. The difficulty to improve the fusion parameter $(\hat{n}_i \cdot \hat{T}_i \cdot \tau_E)$ (and so the ignition margin of a given machine) by the only virtue of additional power is illustrated in Fig.8. The major gains observed in JET result either from temporary changes in the confinement or from increasing the magnetic field and/or the current. If the swcaling laws best describing the energy confinement in JIT continue to apply [2], then a reactor must be very close to ignition without any additional heating power. This means that the required temperatures must be obtained in those conditions; the dependence of radiation and fusion cross-sections imposes in practice an average temperature above 7keV. In addition, density and temperature have not a symmetric effect on confinement: it is easier to get a better energy confinement at high density than at high temperature.

II.3 Particle Transport

Particle and impurity transport in JET have been studied under different operating conditions [3,4]. In most cases, particle confinement, like energy confinement, is anomalous. JET results point strongly towards a common explanation for heat and particle transport. For instance, multi-pellet injection produces peaked high density profiles but flat and low temperature profiles occur in the ohmic regime. Increasing the central electron temperature by on-axis ICRF heating degrades the energy confinement and results mostly in a collapse of the central density (i.e. of the particle confinement). In cases where the collapse is delayed, energy confinement in the plasma centre is also better than in usual additionally heated discharges. The particle confinement time is 5-10 times larger than the energy confinement time.

The anomaly in the particle transport prevents impurity accumulation in the discharge centre. Combined with wall-carbonization, this has kept a low metallic impurity content in JET ($\approx 10^{-4} n_e$) and $Z_{eff}=2$ has been achieved with large additional power. But for most of the discharges the steady state mean value of Z_{eff} ranges between 2 and 4 with a radial profile which tends to peak on axis. Radiation losses in the plasma core are marginal, as long as the dominant impurities are of low atomic number. Under conditions of improved energy confinement, such as H-modes or peak density profiles, impurities are also better confined. Especially in the latter case, the medium- and low-Z impurities seem to accumulate near the plasma axis, showing neo-classical behaviour. This results in an increased deuterium

dilution in the plasma centre and increased central radiation losses.

The scrape-off layer of the JET plasma have been studied under various conditions [5,6]. In limiter discharges, the plasma edge temperature ranges from 25 to 100eV, increasing with the input power and decreasing with density. The scrape-off thickness is typically 1cm; this quantity is invariant under most conditions, except that it increases during ICRF heating. In X-point operation, all atoms and molecules recycling from the divertor near the separatrix are ionised locally.

Consequences for a Reactor

The observation that the particle confinement time is several times the energy confinement time has consequences for the reactivity of the core of the plasma: it will result in a relatively high concentration of impurities and helium. For high Z impurities, the radiation losses may prevent attainment of the required temperature. For low Z impurities, in addition to helium produced by nuclear reactions, dilution of reacting ions will reduce the α-particle power.

The small scrape-off layer thickness results in a high power load on any material in contact with the plasma. This prevents the use of pump-limiters in a reactor in favour of an open divertor to take the plasma exhaust, and will require sweeping the separatrix over the divertor plates to reduce the mean peak thermal load.

II.4 Plasma-Wall Interaction

A variety of materials have been used for wall protection and high heat flux components [7]. JET initially operated with metallic walls, but the inner surface of the vessel (≈200m²) is now more than 50% covered with fine grain and carbon fibre reinforced graphite tiles. The remaining area is carbonised by performing glow discharges with some methane content. The wall temperature is maintained at ∿300°C. If previously conditioned by running discharges in helium, the carbon wall has proved to be a very efficient pump for deuterium during plasma discharges [8]. A variety of models have been proposed but experimental evidence from JET supports the explanation involving co-deposition of hydrogen and carbon in the form of saturated H-C films. It is indeed observed that more than 10-30% of the deuterium introduced into the vessel remains in the form of a deposited layer of hydrocarbons.

The dominant impurities in JET plasmas are carbon and oxygen. Their total amount is controlled mainly by the interaction of the plasma at the limiter. During a discharge, erosion of the limiter material is observed at the point of contact with the plasma and redeposited slightly further outside, as shown in Fig.9. Major plasma disruptions are most efficient in transporting materials from the first wall to the limiter. The ICRF antennae are separated from the plasma by a Faraday shield made of pure nickel. When the ICRF power is turned on metal is released from the screen and can also contaminate the limiters. In absolute terms, the nickel increase is low, especially if the screen has been previously carbonised, but it

is planned to use beryllium in the future to take full advantage of this low Z material.

The increase in additional power and therefore of the heat load in JET has necessitated an increase in the material area in contact with the plasma. Belt limiters are now in use, whose power handling capabilities exceed 40MW for 10s (see Fig.1). For X-point operation, eight graphite poloidal rings were installed to protect the top and the bottom of the vacuum vessel. Water cooled dump plates will be installed during the next shutdown to increase the 40MJ-2s present power handling limitation. Protection tiles have been broken during X-point operation and Fig.10 shows the state of a graphite tile found in the vessel. Needless to say, the falling tile triggered a major plasma disruption. Carbon fibre reinforced graphite has been used in areas where impact of runaway electrons or neutral beams could occur, as these can withstand $30MWm^{-2}$ for a few seconds.

Consequences for a Reactor

The use of low Z material for the plasma facing components seems still to be the best option. Graphite, as used up to now on JET, behaves generally well but problem areas have been identified such as its role as an impurity source, its high chemical reactivity with hydrogen and its high retention of hydrogen leading to problems with density control and with tritium inventory. Combined use of beryllium carbide and of carbon fibre reinforced graphite is a sensible proposal but this is clearly an area where further research is required.

In order to avoid fragile cooling systems in the immediate proximity of the plasma, the heat load at the divertor plates should be limited to $2MWm^{-2}$. To spread the power over a large area and together ease the accuracy required in the shaping of the tiles, the best way seems to sweep the X-point radially.

II.5 Operational Limits

The maximum thermal and mechanical stresses in a tokamak are experienced during plasma major disruptions. The plasma thermal energy is dumped on the limiter and about 50% of the poloidal magnetic energy is dissipated in the vessel walls. The time-scale ranges from 100μs for thermal dump to tens of milliseconds for the dissipation of eddy currents. In addition, runaway electrons are produced in the decaying plasma and can deposit their energy on very small spots (up to $500MJm^{-2}$). When the elongation becomes too large ($\chi 1.8$), a vertical instability can develop followed by a disruption. In this case, with high currents, vertical forces acting on the vacuum vessel have been measured up to 350tonnes.

Major disruptions occur when the power radiated by the periphery of the plasma, around the $q_\psi=2$ surface, exceeds the input power in this area or when $q_\psi=2$ at the plasma boundary. Therefore, they occur preferentially when attempting to increase the plasma density above a limit, which depends on the input power and on the cleanliness of the plasma (see Fig.11) or when attempting to work at a too low q_a value. These can also occur accidentally when a piece of wall material falls into the plasma or subsequent to the crash of "monster" sawteeth

where the released energy induces important outgassing from the wall.

Internal disruptions (or sawteeth) present another limitation in performance which can be achieved in JET. The increased volume inside the q_ψ=1 surface is the most likely reason for confinement saturation observed in JET when $q_a < 4$. Fig.12 shows the saturation of the incremental confinement time τ_{inc}(= $\partial W/\partial P$) when I_p/B(MA/T) exceeds unity in JET (i.e. when $q_a \leq 4$).

So far, JET performance has not been limited by β values that are too high. In experiments performed at 1.4T, and with 10MW ICRF power, the dimensionless factor $g = a.B.\beta/I_p$ has not exceeded 1.6 (i.e. 60% of the Troyon limit).

Consequences for a Reactor

The ignition domain of a reactor must be large enough to avoid operational limits experienced in present days tokamaks. A major disruption at full current cannot be completely excluded and the machine must be able to support the resulting stresses, but repetitive disruptions must be avoided. This means that the required performance should be achieved at $q_a \geq 2.5$ with a reserve in β and with a low enough heat load on the wall. On the other hand, it can reasonably be expected that the ohmic density limit will be overcome in the presence of strong α-particle heating.

Large internal disruptions must also be avoided to ensure a smooth burn of the plasma. By contrast with the present situation, monster

sawteeth could be deleterious in a reactor. This depends upon the steady-state current profile, but operating at a medium value of q_a may be necessary. The size of an ignition device must ensure that the central temperature is large enough even in these conditions to sustain production of fusion power.

II.6 Neutron Yield

Maximum neutron yields approaching $10^{16} n/s^{-1}$ have been observed in JET. Maximum values of Q_{DD} on JET are $\approx 4 \times 10^{-4}$. In a similar 50% deuterium-tritium plasma, the maximum corresponding ratio Q_{DT} would be in excess of 0.1. It must be noted that in these conditions, about half of the neutrons result from reactions between the injected beams at 70/80keV and the target plasma. The other half are produced by true thermonuclear reactions. At low electron density with neutral beam injection, the ion temperature, T_i, significantly exceeds the electron temperature, T_e. Only a combination of NB and ICRF has produced simultaneous high T_i and T_e.

Neutron fluxes in JET have already been sufficient to induce a non-negligible radio-activity of the inner components of the vacuum vessel. When tritium is introduced in JET in 1991, the total value of the ratio Q_{DT} is expected to exceed 0.5. This corresponds to a total nuclear power of about 15MW, taking also into account the beam-plasma reactions. Already, in a D-T plasma, at the achieved temperatures, the percentage of high energy α-particles will be similar to those of a plasma at ignition; it may then be possible to observe the effects of those α-particles in the plasma behaviour and to compare with energetic minority ions created by ICRF.

Consequences for a Reactor

Peak Q_{DD} values achieved in present tokamaks are in an operation mode which is not relevant to an energy producing reactor. These so called "hot-ion" modes cannot be extrapolated towards ignition where the ion temperature should be close to, but lower than, the electron temperature. In a driven system, where the ion temperature could be higher, the recirculating power needed to decouple the ions from the electrons would be prohibitive (see Fig.8).

III HEAT TRANSPORT AND SCALING

The heat and particle transport observed in JET, as well as in other tokamaks, clearly shows anomalous behaviour: the various observed scalings also depend on operating mode. This behaviour has analogies with the appearance of turbulence in fluids. To predict an ignition experiment or a reactor, it is necessary to obtain a plasma description in terms of physics parameters fitting present experiments and allowing calculation of the various temperature and density profiles. This means that the thermal conductivities and the particle diffusion coefficients must be expressed in terms of plasma physics parameters with their proper dimensions. Without even defining local transport, most of the scaling law proposed do not fulfil dimensional constraints.

JET results show a coherence between the anomalous heat conduction of ions and electron and anomalous particle transport. Accordingly, the hypothesis has been made that the anomaly in tokamaks is mainly due to a single phenomenon linked to the topology of the magnetic field. If so, the plasma phenomena of ohmically heated plasma, L-mode, H-mode,

supershot, etc., must be simulated by the same expressions. It was concluded that a critical temperature model fulfilled these conditions.

In this model, when a critical temperature gradient (which depends on local plasma parameters) is exceeded, anomalous transport develops

$$(\nabla T_e)_c = 5.5 \left(\frac{\eta j B_t^3}{n\sqrt{T_e}}\right)^{1/2} \frac{1}{q} \tag{2}$$

and

$$\chi_{an} = 0.6 \left| \frac{\nabla T_e}{T_e} + \frac{2\nabla n}{n} \right| \left(\frac{T_e}{T_i}\right)^{1/2} \frac{R}{r} \left| \frac{q^2}{\nabla q B_t R^{1/2}} \right| \tag{3}$$

where χ is in $m^2 s^{-1}$, T in keV, n in $10^{19} m^{-3}$, B_t in T, lengths are in m, and ηj in V/m; T_e and n_e are the electron temperature and density, T_i the ion temperature, η the plasma resistivity, j the current density, B_t the toroidal magnetic field, and F_e the electron heat flux.

$$\text{If, } |\nabla T| \geq (\nabla T_c), \text{ and } \nabla q > 0$$

$$F_e = \chi_{an}\, n\, |\nabla T_e - (\nabla T_e)_c| \tag{4}$$

In addition, the ions behave in a similar way:

$$\chi_{ian} \sim \chi_{an}$$

$$\text{with } F_i = \chi_{ian} \left| 1 - \frac{(\nabla T_e)_c}{\nabla T_e} \right| n_i \nabla T_i \tag{5}$$

These formulae are still subject to some doubt about β_p dependence as the data are not precise enough, (for instance, a dependence on $\beta_p^{1/2}$ could be

added); the dependence on geometrical factors such as k_i, (r/R), $(\nabla n/n)$ and $(\nabla T_e/T_e)$ is also difficult to determine as the range of variation is relatively small.

The topology of the magnetic field enters through the shear $(\nabla q/q^2)$. Sawteeth have to be taken into account when q reaches unity in the centre.

The behaviour of the heat flow across the plasma can be compared with the flow of water inside a pipe. A transition occurs at a critical value of the pressure when the turbulent flow sets in at the critical Reynolds number (see Fig.13). Eq.(4) describe a similar behaviour for the heat flow in a tokamak when the transition to anomalous transport occurs above a critical temperature gradient.

This specific model gives a general scaling of the following form for the asymptotic behaviour (at high power).

$$\tau_E \propto \beta^{-\alpha} I_p a R^{1/2} \tag{6}$$

$$(nT\tau_E) \propto g_T^{(1-\alpha)} \left(q_a \frac{R}{a}\right)^{\alpha} I_p^2 B_t R^{1/2} \tag{7}$$

where g_T is the Troyon factor and α reflects the uncertainty in the β_p dependence. Eq.(3) corresponds to $\alpha = 0$.

Global scalings are useful but only knowledge of radial profiles allow a proper evaluation of plasma performance. Using Eq.(2-4) in a 1-D transport code, good simulations not only of JET results but also of

other tokamaks have been achieved [9,10].

The main predictions for JET are given in Table III, where only the thermal component of the α-particle production is taken into account. This model has been also used to predict the size of an ignition device and its conditions of operation. It appears that to ignite within a sensible ignition domain, a tokamak with plasma current capability of 30MA and with a toroidal field of 4-5T is required, i.e. the parameters chosen for JIT. Calculations have also been undertaken for various next-step proposals: Ignitor, NET II and ITER. The dimensions and parameters used are given in Table II.

In these simulations, radiation and dilution caused by impurities were taken into account. The hypothesis is that only low Z impurities ($Z \sim 7$) are present, giving 30% radiation of the total heating power (which include the losses due to recycling particles and charge exchange at the edge), in addition to the Bremsstrahlung which is consistently calculated across the plasma.

Sawtooth behaviour inside the $q = 1$ region plays an important role for the ion and electron central temperature. When sawteeth are fully effective, the electron and ion temperature and the current density are flattened inside the $q = 1$ region (see Figs.14, 17(b)). In "monster" sawteeth cases, the temperature of electrons and ions are allowed to develop and the safety factor value is imposed at the centre (see Figs.15, 16, 17(a)). The density profile is not calculated but taken as given by experiment. Generally, this is a relatively flat profile ($\propto [1-(\frac{r}{a})^2]^{\frac{1}{2}}$ or even flatter in H-mode cases.

Improved confinement, mainly due to a peaked density profile, seems unrealistic in a semi-continuous reactor where there are no particle sources to maintain it.

In this model, increased H-mode confinement is due to pedestals developing in regions of very high shear near the separatrix, but the main core of the plasma behaves as an L-mode (see Fig.16). At high power, gains from the H-mode might disappear as the relative influence of the separatrix weakens. Taking into account impurity behaviour, a stationary H-mode has not yet been found experimentally, which precludes considering its enhanced confinement for a reactor. When ELMs are present, operations closer to steady state have been observed, but are generally associated with a partial loss of confinement. Nevertheless, in a transient way an improved confinement regime (H-mode, monster sawteeth) could be useful to ease the transition to an ignited plasma.

Predictions for proposed future experiments are given in Tables IV and V. In those tables, the factor g does not include the pressure generated by the α-particles and brackets indicated that the additional power has been switched off when the α-particle power has reached sufficient level. No bootstrap current has been included.

One conclusion of the simulation is that it is extremely difficult to vary the electron temperature (and consequently the ion temperature) in a tokamak, without involving heating power larger than the α-particle heating. In other terms, ignition could almost be reached without additional heating; only a modest level would be required in a machine like JIT (25-50MW). The increase in thermonuclear power is realised by increasing the density at almost constant temperature (see Fig.17).

The cases labelled "ohmic and α with monsters" in Table IV and V, can be used to compare the predicted ohmic performances of the various machines. Compact high field machines generally suffer at high densities from an insufficient temperature giving rise to a high level of bremsstrahlung and to a low reactivity, even if the confinement appears good (see Fig.15). In general, except in JIT, sawteeth are able to destroy ignition at low q. NET II should behave almost as JIT and therefore has a larger ignition margin than ITER, if technology development is sufficient to permit the parameters in Table II to be reached (see Fig.17).

This code also predicts that, with monster sawteeth or with an H-mode pedestal at relatively low density, JIT could reach ignition without additional heating.

IV POSSIBLE NEXT STEP TOWARDS A DEMONSTRATION REACTOR (DEMO)

IV.1 Reactor Studies

Reactor studies show that the thickness of the blanket and shielding inside the coils, e_b, should exceed 1m (i.e. 1.5-2m). To use the magnetic field efficiently, the plasma radius, a, should be greater than $2(e_b+e_c/3)$, where e_c is the toroidal coil thickness; this gives as a minimum size of a=3m [11]. With a toroidal field of 4-5T, and an elongation of 2, the plasma current capability of such a machine should be over 30MA. Such a reactor should be able to ignite in the L-mode without problems of confinement. It can be seen that too high confinement might even have a negative impact on the impurity level and on the exhaust of the helium produced; the rate of diffusion of helium towards the wall and of fuel towards the centre needs to be

fast enough to maintain the plasma reactivity. Already a particle diffusion coefficient 5 times lower than the heat diffusivity, as it is observed on JET, will affect the power output of the reactor.

IV.2 Questions Relating to First Wall and the Plasma

Before a power reactor can be built, the following problems involving the plasma and the first wall still need to be solved:

1. plasma wall interactions: fuelling, exhaust and level of impurities;

2. concept of the first wall with the high heat transfer elements, erosion of the limiter and divertor plates, and retention of tritium within the first wall;

3. necessity of maintaining smooth operations free of disruptions, giant sawteeth, collapse of H-modes, etc.

IV.3 Next-Step Device

A next-step device could be aimed at producing a full reactor plasma reactor and at demonstrating that solutions for the first wall and smooth plasma operations could be found. Such a plasma will require a very long burn ($\sim$30 mins) and a high duty cycle (semi-continuous operation). Such requirements mean that it will also be possible to test the concept of different blankets for DEMO. This specific choice allows a large ignition domain depending on q and on plasma density: the power produced could vary in the range 500-4000MW. The

best way to reach ignition appears to start with a plasma at a relatively low density with a moderate current of 25MA and to increase the density and plasma current when ignition is reached to produce a power level of several GW (similar to that of a reactor). This should demonstrate the potential of fusion as an energy source. Such a device is referred to as a "thermonuclear furnace" and a possible choice of parameters (JIT) is given in Table VI.

IV.4 Semi-Continuous versus Continuous Operation

One of the questions which has an overall impact on the choice of solution and on the very concept of a reactor is that of the necessity of continuous operation, which seems almost incompatible with the concept of ignition.

In a reactor, the central temperatures should reach 25keV or more and therefore the voltage per turn will be extremely low ($\sim$0.05V or less). Flux consumption of 100V.s during the flat-top will ensure a burn time of more than 30 mins which could even exceed 1 hour in the presence of bootstrap currents near the beta limit. A high duty cycle could be obtained by reversing the plasma current when the transformer has reached saturation.

Continuous operation of a tokamak is more complex in terms of physics and equipment. High energy neutral beams or radio-frequency techniques are required to drive the current. However, the efficiency of non-inductive current drive is quite low compared to the use of a transformer and the gain in the duty cycle may not be significant. In addition to the cost and the complexity of equipment

needed for current drive, the recirculating energy would also increase the overall cost of electricity produced by an amount which could become a dominant factor and condemn such a concept.

On the other hand, semi-continuous operation requires a moderate intermediate thermal storage or a set of tokamak-reactors working together. The main advantage of continuous operation is to reduce the thermal fatigue of components inside the reactor but as long as the burn time is longer than 1 hour this may not be important.

In conclusion, semi-continuous operation with long burn for a next-step device seems to be a proper solution taking into account the complexity of non-inductive current drive and its doubtful relevance for a reactor.

IV.5 Tritium Consumption

The consumption of tritium is proportional to the energy produced 5.5g/GW_th; it is also proportional to the product of the fluence and the surface area of the walls. If a certain fluence is required for testing blanket elements of a given dimension, and if parallel testing of different blankets can be done, the consumption of tritium will be equivalent for various machines. If parallel testing cannot be done, the consumption of tritium will be proportional to the surface area which may not vary more than a factor 2 between different concepts of next-step device.

To maintain simplicity and considering the duty cycle and tritium consumption in the next machine, a breeding blanket seems an

unnecessary complication for an apparatus which is unlikely to test any blanket material at high neutron fluence. For the next step, although some test modules of breeding blankets could be introduced, only neutron shielding has to be provided.

IV.6 Conclusions on a Next-Step Device

In conclusion, the next generation of tokamaks must demonstrate that an ignited and burning plasma at high power with semi-continuous operation can be realised.

The aims of such an experiment could be:

- to study the ignition domain;
- to test wall technology;
- to test some breeding blanket modules for DEMO;
- to demonstrate the potential of fusion as an energy source.

From JET results, such a machine can be defined, but it requires a large ignition domain to operate safely with minimum scientific risks. In the same spirit, technical risk for the apparatus must be kept low and the simplicity of the concept must be paramount.

V DESCRIPTION OF THE THERMONUCLEAR FURNACE

V.1 Introduction

The main design characteristics of a thermonuclear furnace (JIT) to meet these objectives are presented, of which the main priorites are simplicity and sturdiness of concept. Basically, the plasma

parameters are scaled up from JET by a linear factor of 2.5 and several elements of the JET concept are maintained.

To minimize technical risk, size of the coils, shielding and overall cost, water cooled copper magnets are proposed but superconducting magnets could be envisaged, if advantages compensated for the extra complexity. Low current density is used in the water-cooled copper coils to allow continuous operation. A large flux swing ($\gtrsim$400V.s) would also provide the necessary drive to maintain the flat-top currents for periods up to one hour.

A general view of the apparatus is given in Figs.18 and 19. It should be noted that the magnetic circuit is also used as a radiation shield around the machine.

V.2 Vacuum Vessel, Toroidal Coil, Mechanical Structure

The device concept is based on a highly integrated and modular construction where all the elements would be manufactured on-site, as transport of components of this size would not be possible.

The machine basically consists of 20 sectors supported radially by a cylinder formed by the ohmic transformer. Each of these sectors integrates the toroidal coil, the vacuum vessel and the mechanical structure (see Fig.20). These different sectors are assembled together by welding flexible lips. The torque induced by the vertical field is taken in shear by the light structure which encloses the toroidal coil. This structure around the toroidal coil is sufficiently thin to allow the plasma current to penetrate through

the torus. An insulated mechanical element on the external part of the coil directly transmits the shear forces.

The coils are made of a single pancake of water cooled copper corrugated in order to transmit the shear forces while the insulation remains purely in compression (see Fig.21). This feature would allow the use of a purely inorganic insulator for insulation of the coil inner turns, making it possible to withstand high radiation levels. At 4.5T toroidal fields, the power dissipated in the coil would be 1.3GW and the stresses in the copper or in the vacuum vessel structure remain at an acceptable level.

V.3 Poloidal System

The magnetic configuration contains a single null X-point (see Fig.22), where the X-point is located in the lower position to allow the foundations to take the extra forces resulting from the presence of the separatrix giving more access at the top of the machine. This position also decreases the risk of broken tiles falling into the plasma. The presence of the X-point would allow transient H-mode operation during the transition to ignition, but its main purpose is to provide pumping of the plasma at relatively high pressure.

The position of the poloidal coils is similar to that in JET. The coils are Bitter type and made by sectors of thick copper plates (3-4cm) welded together (see Fig.23). Water flowing through holes perpendicular to the plates provides essential cooling. The insulation is not bounded and the whole could be immersed in water. These coils are supported by a magnetic circuit which also provides

radiation shielding. The magnetic circuit is conceived as a massive metallic building. This concept allows the use of ordinary concrete for the foundations and the other elements of the external building.

The total flux swing of the ohmic transformer is 420V.s and the maximum resistive consumption is ∿350MW. The flux needed to establish the magnetic configuration at 30MA is 270V.s leaving 150V.s for resistive dissipation during the start-up phase and flat-top. Table IV shows that the loop voltage during flat-top could be as low as 0.04V.

V.4 Internal Shielding and First Wall

The shielding is made of several elements which could be dissassembled remotely without dismantling the main apparatus (see Fig.24(a) and (b)). Each of these elements is made of a single box structure filled with pebbles of metal directly cooled by water (see Fig.21). One of the main problems in maintaining shielding efficiency is the presence of gaps to allow remote handling and thermal expansion of the different elements. These gaps reduce the shielding locally and could permit a high neutron flux to reach the coils. The overall layout includes a series of thicker elements which could easily be replaced by reactor relevant breeding-blanket test modules (see Fig.24) without any modifications of the initial shielding and of the plasma parameters.

The first wall itself is formed by the surface of the shielding box facing the plasma with only local protection by carbon tiles which radiate energy received at a temperature ∿1500°K. These tiles would

serve as a protection against disruptions from runaways and would mainly cover the inner wall and top and bottom of the machine.

A continuous deposition of beryllium could ensure that the first wall seen by the plasma is of beryllium or its carbide. This would help to limit sputtering and outgassing of the tiles. This design does not present major problems at a load of 2MW/m² for the fusion power produced. The main parameters of the first wall are given in the Table VII.

V.5 Divertor

The divertor presents the main technical challenge in the design of inner wall components. This challenge can be reduced to a managable level if the region of high power deposition is expanded over a larger area. This can be achieved by moving the X-point vertically or horizontally using the existing coil set or preferably by using a set of internal saddle coils. Alternatively, the movement could be achieved by oscillating divertor components horizontally. The main advantages of this scheme would be:

- no need to position the divertor components with mm accuracy (as required in JET) and a feed-back technique could be used;
- in spite of high local thermal loads, the average load remains small;
- heat transfer to the cooling medium corresponds to the average load;
- lifetime increases by reducing the ratio of peak load to average load:
- to compensate for erosion, material (beryllium, hydrocarbons) could be injected;

- deposited and redeposited layers are burned off before they can flake and before large amounts of tritium could accumulate.

For the movement, the limiting factor is the sweep frequency which should be low enough to allow a relatively simple set of additional coils in the vacuum vessel, but on the other hand, should be high enough to minimize thermal stresses in the divertor material.

Fig.25 shows a cross-section through the divertor region, in which the divertor plates extend above and below the X-point. These receive only a moderate average power level of $1.3 MWm^{-2}$ from radiation and conduction. The X-point can be moved horizontally by local saddle coils. The target tiles intersect the magnetic flux surfaces at a small angle of incidence and therefore a small radial displacement of the X-point allows a distribution of the power load over the whole divertor surface.

The material proposed for the divertor plates is 40mm thick carbon fibre graphite. It is brazed in $10x10 mm^2$ surface area blocks to water cooled copper plates of 10mm thickness. The average heat flux (conduction plus nuclear heating) is $\sim 1.8 MWm^{-2}$ which could be removed without having to resort to two phase cooling. In the proposed design, peak surface loads during the sweeping of the X-point would be about a factor of five higher than the average load ($\sim 10 MWm^{-2}$). For the calculation of thermal response, the high thermal conductivity of the fibre graphite was not taken into account as it degrades at low neutron doses ($\sim 10^{20} cm^{-2}$) to that of fine grain graphite [12]. For a sweep frequency of 1Hz, surface thermal stresses would be about 25MPa in compression (limit 100MPa) and the

peak temperature would be ∿1400K. The material thickness is mainly limited by the average load and the resulting front temperatures.

It is proposed to continuously cover the graphite divertor with a thin layer of beryllium to take advantage of the good properties of both materials. A beryllium carbide layer would be formed [13] at temperatures above 700K. It is envisaged that such a scheme will be confirmed in JET.

The lifetime of the divertor plates would be determined by the erosion due to particle impact. A detailed modelling of the plasma edge and the divertor region is required to assess particle fluxes and energies. This is presently not yet available. Therefore, a worst case assessment is made. The energy (∿300eV) and the temperature (∿750K) of the maximum sputtering yield is taken for the sputtering of carbon by deuterium. When smaller than unity, the self sputtering of the divertor plates is one of the mechanisms which determines the redeposition rate [7].

Neglecting any increase in lifetime of up to a factor 3-10 due to lower particle energy, possible suppression of chemical activity and redeposition, the lifetime should be at least two months of continuous operation at a level of 2.5GW of thermonuclear power. The pumping is carried out by cryopumps with charcoal.

V.6 Auxiliaries and Buildings

1. Additional Heating

As has been seen in the simulation, JIT could reach ignition with ohmic heating alone during monster sawteeth or in the H-mode

regime. Nevertheless, it would be prudent to consider a moderate level of additional heating of ∿50MW, which could be ion cyclotron heating (analogous to that in JET). This power would only be used in a transient way (with increased efficiency to that in JET): the power density is lower and the coupling would be improved as more room would be available for the antennae. The radio frequency antennae would be an integral part of the shielding and vacuum vessel in the outer regions. This choice also ensures that the centre of the plasma could be heated.

2. Tritium Plant

Little study has been done on the tritium plant but a modest upgrade of the JET tritium plant should be sufficient to feed the machine. The pumping is done using cryogenic techniques for hydrogen isotopes as well as for helium. Extra elements for the detritiation of the cooling water might be necessary. As a full breeding blanket is not envisaged, there is no corresponding plant.

3. Building - Cooling Plant

The first concept of the building to house such an experiment is shown in Fig.19. This building includes all the facilities for remote handling, maintenance and dismantling.

The cooling power for such an installation must have a peak capability of 6GW, but a much lower average requirement. The method of achieving such cooling depends strongly on siting. The

preferred solution would be to take cold water from a lake or sea. The hot water produced during the peak operations could be stored temporarily.

V.7 Cost and Time-Schedule

An approximate cost for such an experiment has been derived from data collected at JET. The cost of the main components is shown in Table VIII, which does not include the test blanket modules. This brings the total construction cost to a value close to 2000MioEcu (1988) without contingencies. Including contingencies and overall cost; 2500MioEcu seems realistic.

Up to 400 professionals over a period of 8 years might be necessary to construct such a device.

VI SUMMARY AND CONCLUSIONS

In conclusion, JET has proved to be a highly successful European collaborative Project. The Project is now midway through its experimental phase, during which its achievements have been significant and has placed it as the major experiment in world fusion research. It is now well set to demonstrate substantial α-heating in a thermonuclear plasma.

The main conclusions are:

1. Plasmas of a thermonuclear grade have been obtained in JET but a large step is still required to reach ignition.

2. JET data shows that a tokamak with a plasma current capability around 30MA is required to produce ignition of a D-T plasma in a practical domain. With lower values of current, the risk of not achieving ignition is large, if sawteeth, impurity radiation, dilution etc., are taken into account.

3. In an optimized reactor, the size would be defined by the blanket and this leads to a tokamak with a current capability greater than 30MA.

4. Confinement would no longer be the dominant problem. However, major uncertainties are in the areas of plasma-wall interaction, fuelling, exhaust and impurity control.

5. Technical considerations of stress level, wall loading and economy result in a concept of a "Thermonuclear Furnace" producing a thermal output of several GW in semi-continuous mode.

6. This device is aimed at demonstrating the potential of a Tokamak Reactor and to test wall technologies and breeding blankets.

7. For such a device, priority must be given to the simplicity and reduction of technical and scientific risks.

If a European programme is to continue, it is important to build on JET achievements and retain and utilize the skills and expertise of its staff as well as their dedication to demonstrating controlled fusion power. To meet these objectives a next step must be conceived which clearly

establishes the potential of fusion as a major source of power. Such a device must give a high priority to simplicity of design with minimal technical and scientific risks. It is a Thermonuclear Furnace of several GW. JIT is such a device which seems compatible with the technical and financial capabilities of Europe and would prove that fusion is potentially a major source of future world energy.

VII ACKNOWLEDGEMENTS

The scientific and technical achievements of JET result directly from the dedication of the JET Team [2]. We also wish to thank Drs. K.J. Diëtz, B.E. Keen, B. Keegan, E. Lazzaro, T. Molyneux and L. Sonnerup for their help in preparing this paper and calculating some elements of JIT.

REFERENCES

[1] Rebut, P.H., et al, Fusion Technology, 11, pp13-281 (1987);

[2] Gibson, A. and the JET Team, "Plasma Performance in JET: Achievements and Projections", 15th European Conference on Controlled Fusion and Plasma Heating (Dubrovnik, Yugoslavia, 1988) to be published in Journal of Plasma Physics and Controlled Fusion;

[3] Gondhalekar, A, et al, "Simultaneous Measurements of Electron and Particle Transport in JET"; 15th European Conference on Controlled Fusion and Plasma Heating (Dubrovnik, Yugoslavia, 1988), Europhysics Conference Abstracts, Vol.12B, p151;

[4] Behringer, K., et al, "Impurity Transport in JET during H-mode, Monster Sawteeth and after Pellet Injection"; 15th European Conference on Controlled Fusion and Plasma Heating (Dubrovnik, Yugoslavia, 1988), Europhysics Conference Abstracts, Vol.12B, p338;

[5] Tagle, J.A., et al, "The Effect of Edge Temperature on Impurity Production under a Range of Operating Conditions in JET"; 14th European Conference on Controlled Fusion and Plasma Physics (Madrid, Spain, 1987), Europhysics Conference Abstracts, Vol.11D, p662;

[6] Kock, L., et al, Role of the Scrape-off Layer in X-Point Discharges in JET; 15th European Conference on Controlled Fusion and Plasma Heating (Dubrovnik, Yugoslavia, 1988), Europhysics Conference Abstracts, Vol.12B, p655;

[7] Rebut, P.H., Diëtz, K.J. and Lallia, P.P., "Experience with Wall Materials in JET and Implications for the Future"; 8th International Conference on Plasma Surface Interactions in Controlled Fusion Devices (Jülich, F.R.G., 1988), to be published in J. Nucl. Mater. (see JET Report JET-P(88)21);

[8] Cohen, S.A. and the JET Team, "Particle Balance and Wall Pumping in Tokamaks", Controlled Fusion and Plasma Physics, 29, 1205 (1987);

[9] Rebut, P.H., Lallia, P.P. and Watkins, M.L., "Analysis on JET Results and Impact for the Future", 12th IAEA Conference on

Plasma Physics and Controlled Nuclear Fusion Research, Nice, France, 1988) to be published;

[10] Taroni, A., et al, "Global Power Balance and Local Heat Transport in JET", 12th IAEA Conference on Plasma Physics and Controlled Nuclear Fusion Research (Nice, France, 1988) to be published;

[11] Reynolds, P. and Worraker, W.J., Study of the Reactor Relevance of the NET Design Concept, Culham Laboratory Report; CLM-R278 (1987);

[12] Kelly, B.T., "Physics of Graphite", Applied Science Publishers, London and New Jersey, 1981;

[13] Nich, T.G., et al, Scripta Metallurgica, 20 (1986) 87;

TABLES

Table I
Major enhancements to JET carried out in 1987

Extensive improvements to the main poloidal circuit to give: improved X-point operation improved control of current rise phase increased volt-second capability	Second NBI box *(first injection, into JET May 1988)* Cryo pellet injection system *(single pellet using Garching gun; multiple pellet using ORNL gun, in collaboration with US–DOE)*
New dual belt limiter system *(carbon tiles on a water cooled base)* plus, carbon tiles on all exposed surfaces *(specially shaped at X-point target)*	Improved vessel mechanical restraints for disruption protection
Eight ICRF antennae between the belts *(water cooled carbidised nickel Faraday screens; carbon side tiles)*	Increased diagnostic capability, especially: Time of flight laser scatter system **(LIDAR)** to measure $T_e(r)$; $n_e(r)$ Faraday rotation polarimeter to measure $B_\theta(r)$

CR88 601

Table II

Main parameters of various devices simulated with the 'critical temperature' code

	R	a	k	B_t	Add.Power	I_p
	m	m		T	MW	MA
JET	3	1.2	1.7	3.4	40	7
ITER	5.8	2	2.2	5.1	100	20
JIT	7.5	3	2	4.5	50	30
Ignitor	1.16	0.43	1.8	14	10	12
NET II	6	2.2	2.2	5.4	50	27

C CR88 106

Table III

Predictions for JET; 'critical temperature' simulations

Device	I_p (MA)	n_{e0} ($10^{19}m^{-3}$)	Z_{eff}	P_{add} (MW)	T_{i0} (keV)	$\bar{T}_e$ (keV)	P_α (MW)	g	P_{OH} (MW)	Regime
JET	7	7.5	2	0	3.5	2.6	0.014	0.24	5.6	ohmic q = 1
	7	7.5	2	40	12	5.2	2.2	1.22	3	monster L-mode q = 0.8
	7	7.5	2	40	5.6	3.7	0.5	0.86	3.2	L-mode q = 1
	6	7.5	2	20	11	5.2	2	1.6	1.4	H-mode + monster q = 0.8: Pedestal T_e = 1.5 keV
	7	4	2	20*	25	5.8	2.5	0.94	2.1	Hot ion L-mode monster q = 0.8

*NBI heating; 80% of the power coupled to ions.

J CR 88 158.4

Table IV

Predictions for JIT using 'critical temperature' simulations

Device	I_p (MA)	n_{e0} ($10^{19}m^{-3}$)	Z_{eff}	P_{add} (MW)	T_{i0} (keV)	$\bar{T}_e$ (keV)	P_α (MW)	g	P_{OH} (MW)	Regime
JIT	30	5	2	0	5.6	3.9	0	0.25	18	ohmic without α (q = 1 sawteeth)
	30	5	2	0	25	11	90**	0.77	5.5	ohmic + α monster q = 0.8 **Ignited**
	20	10	2	(50)*	29	15	511	3	0.75	L-mode Sawteeth (q = 1) **Ignited**
	20	10	3	50	10	5	51	1	5.9	L-mode Sawteeth (q = 1)
	20	10	3	(50)*	32	12	262	2.3	20	L-mode Monster **Ignited**

* Brackets indicate that P_{add} has been switched off when P_α was large enough.
** P_α still rising.

Table V
Predictions for different experiments;
using 'critical temperature' simulations

Device	I_p (MA)	n_{e0} ($10^{19}m^{-3}$)	Z_{eff}	P_{add} (MW)	T_{i0} (keV)	$\bar{T}_e$ (keV)	P_α (MW)	g	P_{OH} (MW)	Regime
ITER	20	15	2	100	18	11.7	300	2.1	1.9	L-mode Q = 15 q = 1
	20	15	2	(100)*	30	13.2	380	2.4	2.2	L-mode monster q = 0.8 **Ignited**
	20	5	2	0	9.8	4.5	4.5	0.27	9.8	Ohmic + α monster, q = 0.8 Q = 2.3
NETII**	27	5	2	0	13	6.3	13.3	0.3	11	Ohmic + α monster Q = 6
Ignitor	12	100	2	10	9.2	4.4	11.6	0.7	25	Monster Q = 1.7
	12	100	2	0	8.2	4	8.3	0.62	27	Ohmic + α Monster Q = 1.5

* Brackets indicate that P_{add} has been switched off when P_α was large enough.
**At 27MA NETII ignites with 50MW of additional power.

J CR 88 158.2

Table VI
Main Parameters of a Thermonuclear Furnace (JIT)

Plasma minor radius (horizontal)	(m)	3
Plasma minor radius (vertical)	(m)	6
Plasma major radius	(m)	7.5
Plasma aspect ratio		2–2.5
Flat top pulse length	(s)	1000-4000
Toroidal field (plasma centre)	(T)	4.5
Plasma current	(MA)	30
Volt seconds	(Vs)	425
Additional heating	(MW)	50
Fusion power	(MW)	500–4000

P CR88.48.1A

Table VII

JIT: Loads on Wall Components at 3 GW(th)

Surfaces		
Wall	(m^2)	1660
Divertor (swept)	(m^2)	190
Wall loads		
Nuclear heating (graphite)	($MW\,m^{-3}$)	12
Radiation	($MW\,m^{-2}$)	0.2
Neutron flux	($MW\,m^{-2}$)	1.5
Divertor loads (when swept)		
50% radiation on 300 m^2	($MW\,m^{-2}$)	1
50% conduction on 200 m^2	($MW\,m^{-2}$)	1.5
Nuclear heating (graphite)	($MW\,m^{-3}$)	12

J CR 88 158.3

Table VIII

JIT: Cost Estimate

Machine			
	Poloidal coils	165	
	Toroidal coils	261	
	Vacuum vessel	64	
	Shielding, First wall	100	
	Mag. circuit	60	
		650	MECU
Auxilliaries			
	Building	200	
	Heat Exchanger	150	
	Tritium Pumping	70	
	Remote Handling	50	
	Power supply	150	
	Additional heating	180	
	Control	150	
		950	MECU
	Machine	650	
	Auxilliaries	950	
	Personnel	200	
	Total	2000	MECU
	Contingencies 20%	400	MECU

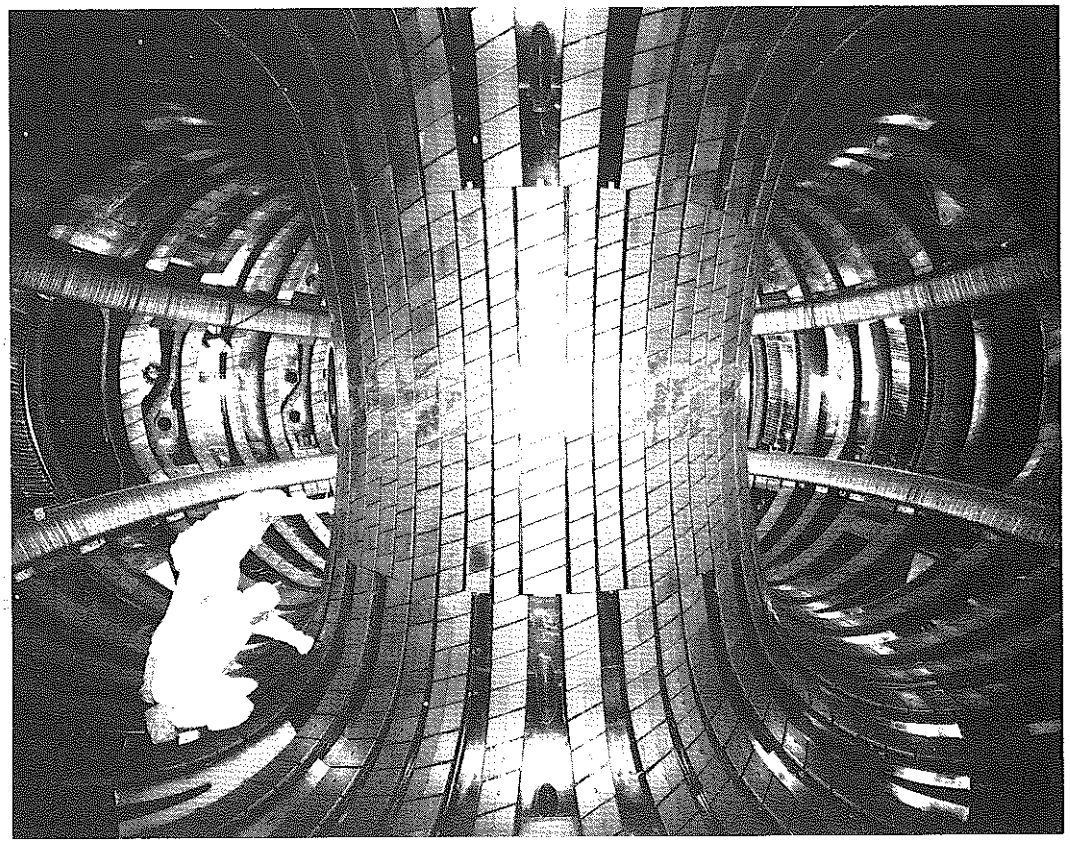

Fig. 1 Status inside the JET vacuum vessel after the 1987/88 shutdown. A large fraction of the vessel was covered with carbon tiles and the metal surfaces were blackened by carbonization. The inner wall protection tiles, the bottom tiles on which the separatrix lies, the belt limiter, the antennae and their protection frames are shown.

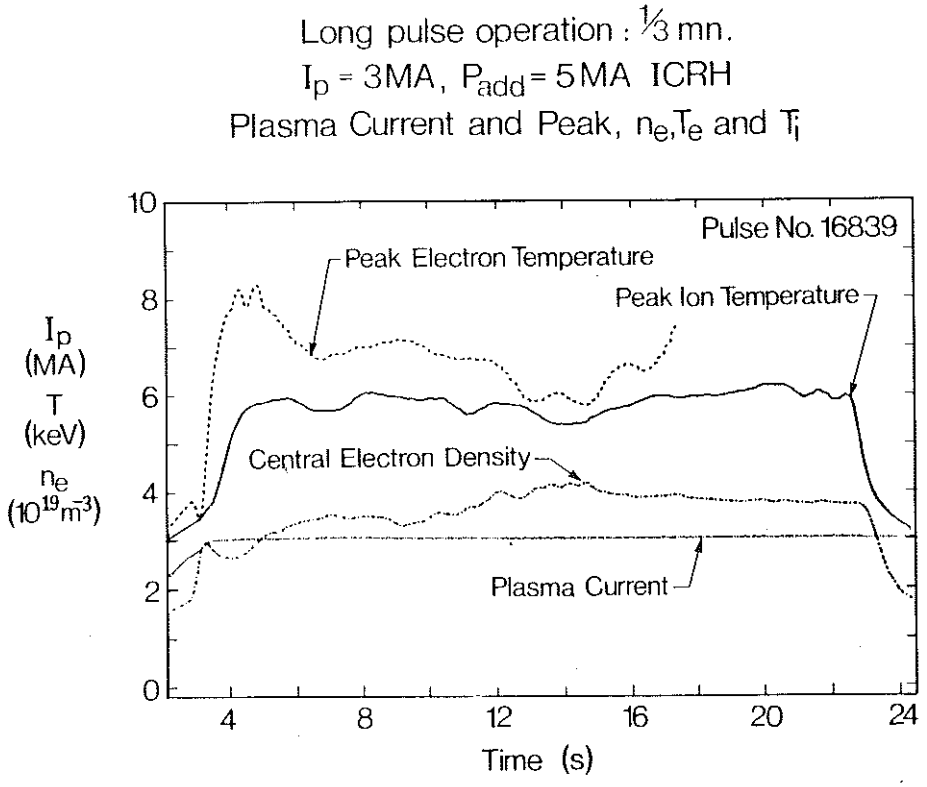

Fig. 2 Quasi-stationary plasma of duration exceeding 30s at temperatures in excess of 5 keV. The 3 MA plasma was heated by 5 MW ICRF power.

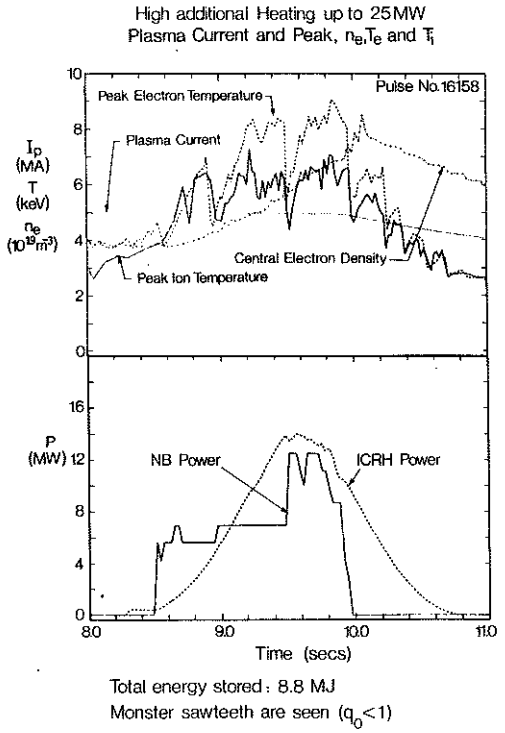

Fig. 3 Evolution of a 5 MA plasma when heated with additional power reaching 25 MW, as shown in the lower figure. The toroidal field is 3.2 T and the stored energy is 8 MJ. The presence of giant sawteeth during the heating is clearly seen.

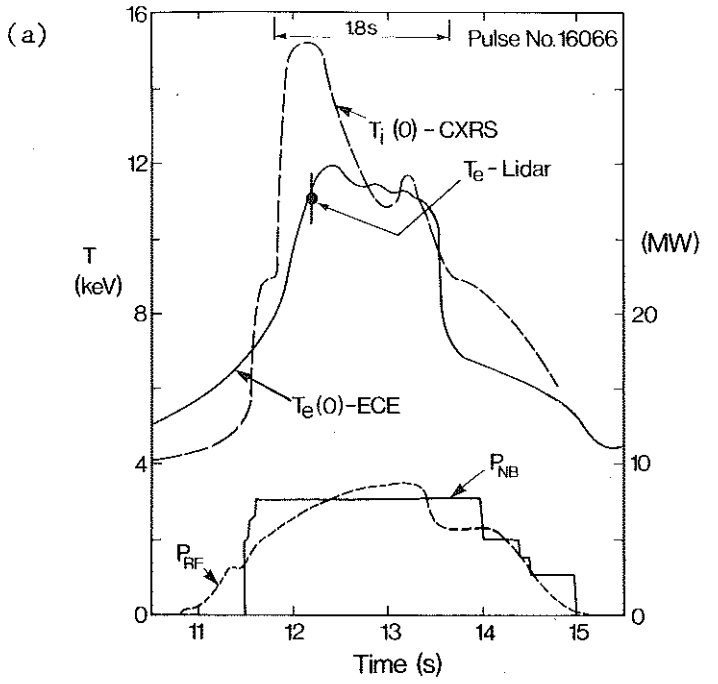

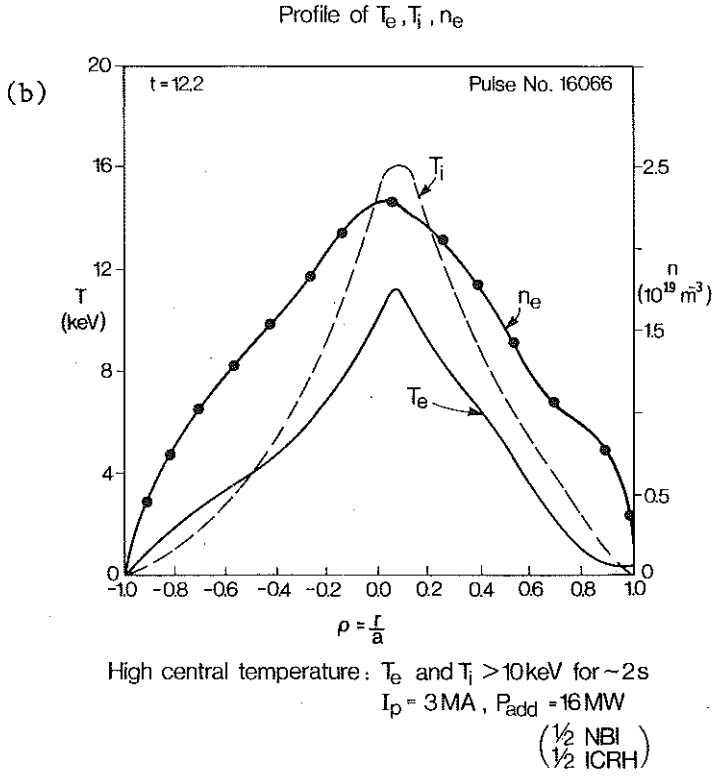

Fig. 4 (a) Peak electron and ion temperatures as a function of time during RF and NB heating; (b) Density and electron and ion temperature profiles at 12.2s for the same pulse No. 16066, which was a double-null X-point plasma at $I_p = 3$MA, $B_0 = 3.2$T.

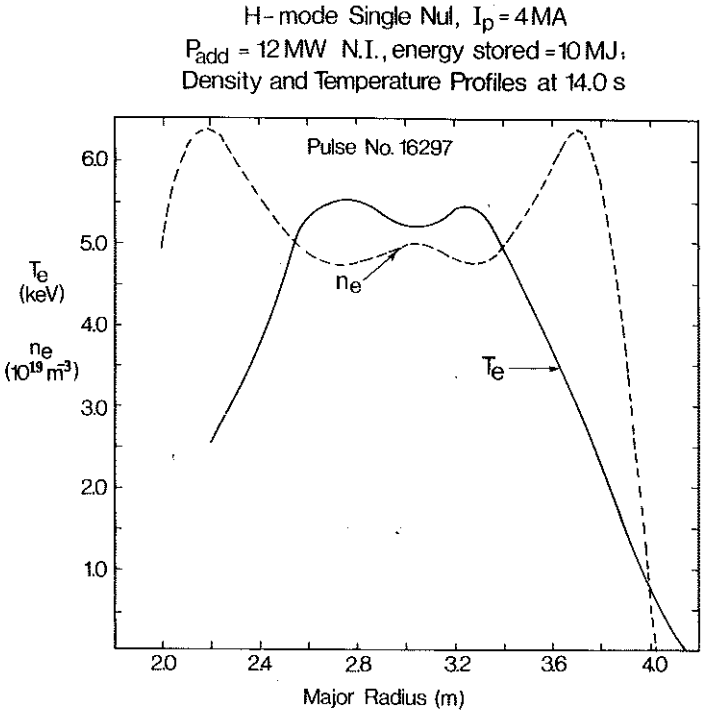

Fig. 5 Density and temperature profiles for a 4 MA H-mode plasma with a confinement time reaching 1 s. The fusion product ($n_D\ T_i\ \tau_E$) reached 3.4×10^{20} m^{-3} keV s. It should be noted that the density profile is hollow and that a temperature pedestal is not apparent (may be due to poor radial resolution (~10 cm)).

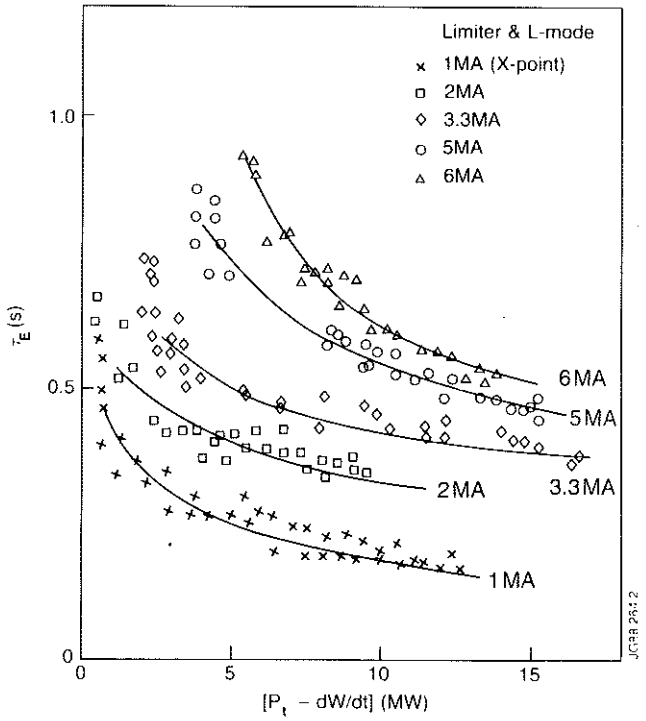

Fig. 6 L-mode confinement time, τ_E, data versus input power, showing degradation with power. The strong degradation of confinement time and the beneficial effect of plasma current is clearly seen.

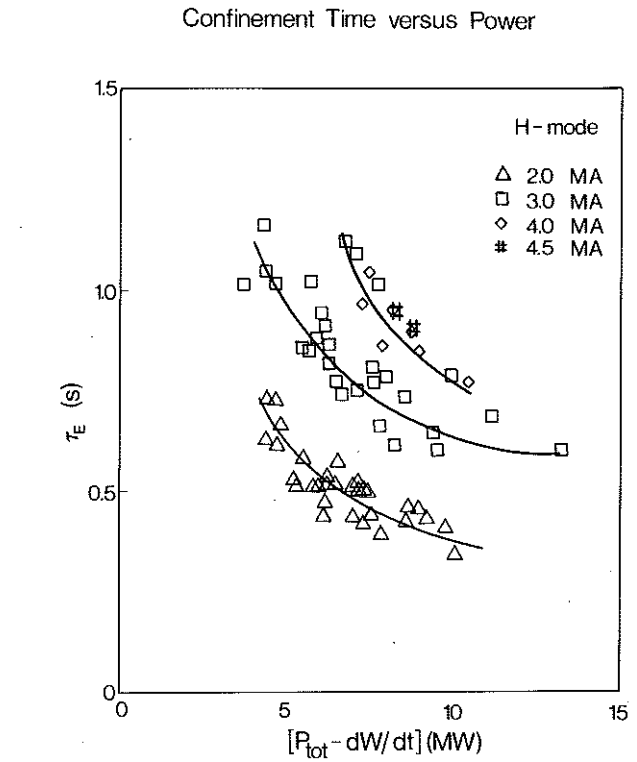

Fig. 7 H-mode confinement time, τ_E, data versus input power showing clear degradation with power. However, confinement is improved by a factor 2 to 3 over the corresponding L-mode case.

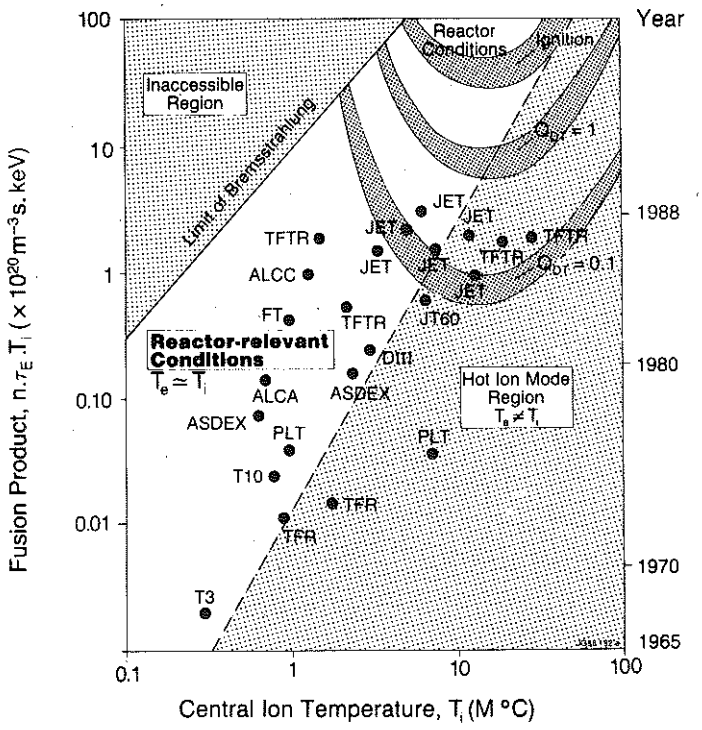

Fig. 8 Fusion parameter as a function of central ion temperature for various fusion devices. The mode of operation relevant for a reactor is where the electron and ion temperatures are nearly equal at values between 15 and 50 keV. The high density/low temperature region is forbidden due to radiation losses.

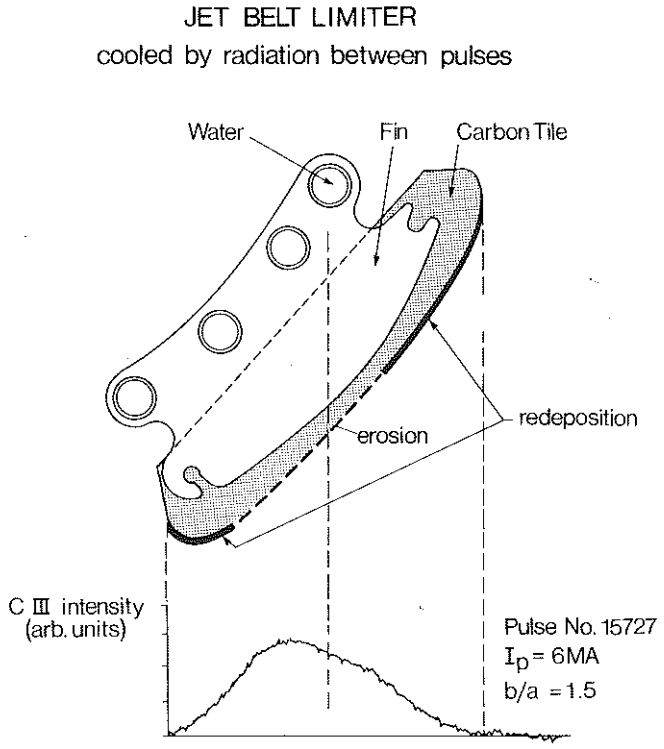

Fig. 9 Cross-section of the belt limiter with radiating tiles on water cooled fins. The carbon intensity is shown together with erosion and redeposition zones.

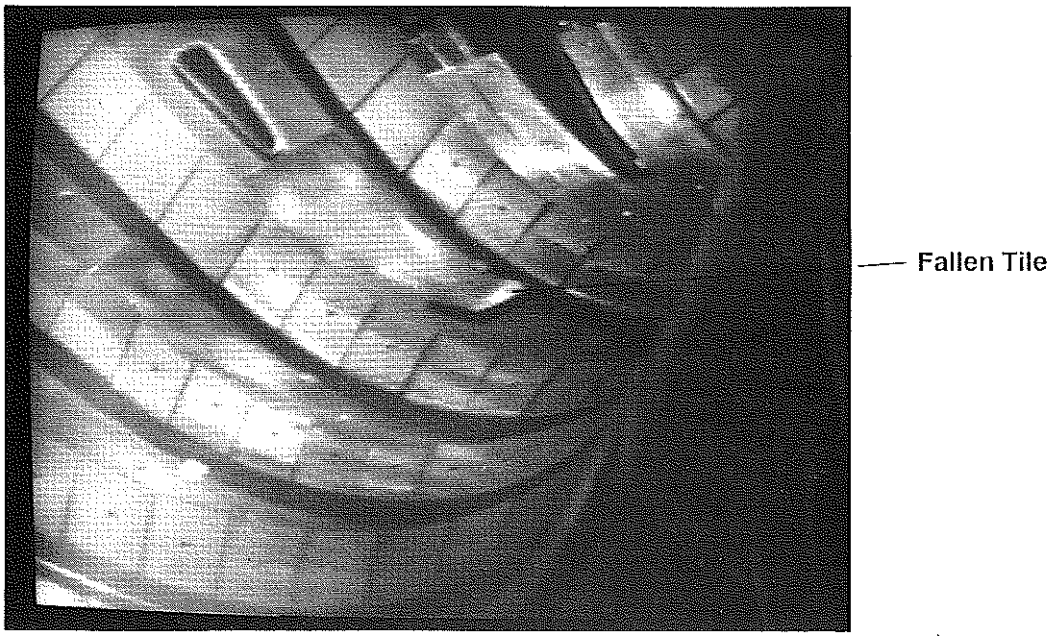

Fig. 10 Picture of the bottom of the JET vacuum vessel taken with a remote handling viewing system. A graphite tile which failed during X-point operation is shown.

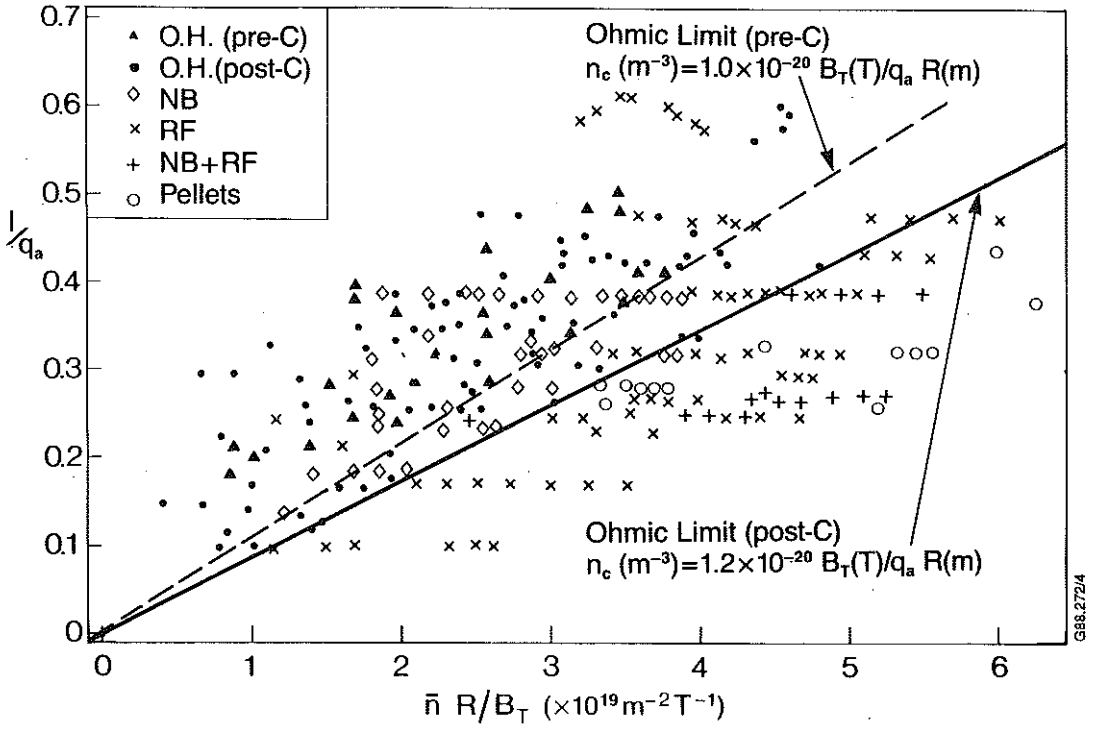

Fig. 11 Shows the Hugill diagram for the density limit. The limits for ohmic discharge without carbonisation, and with carbonisation (low Z) are indicated. Pellets and additional heating allow a higher density to be reached before a disruption occurs.

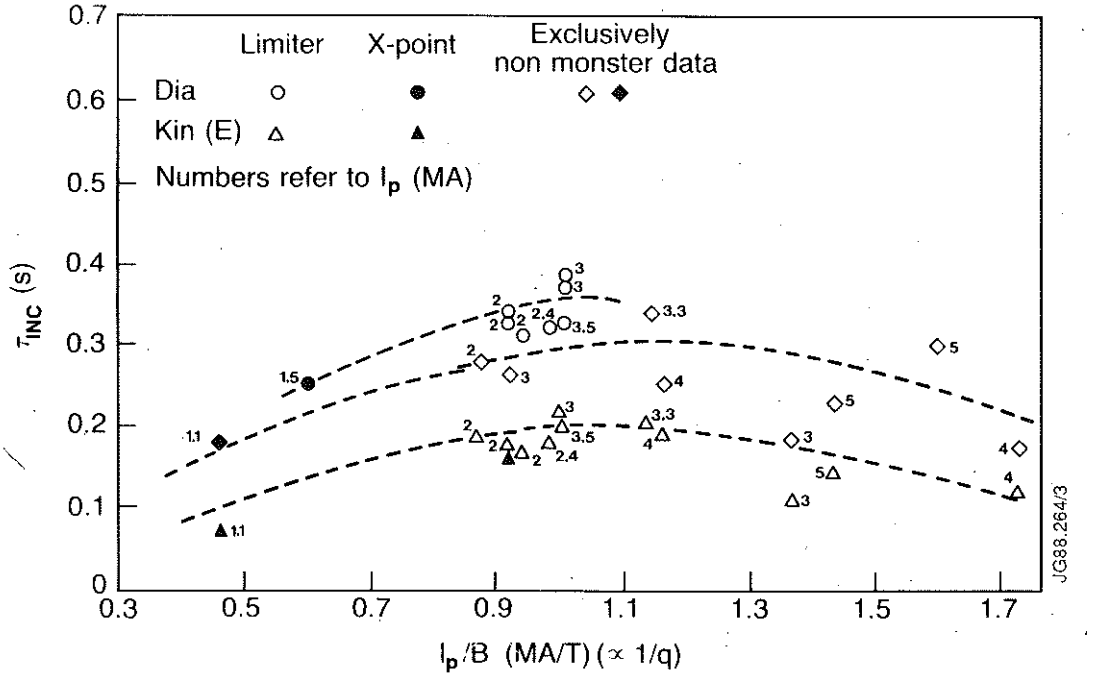

Fig. 12 Incremental confinement time, τ_{inc} ($=\partial W/\partial P$) as a function of (I_p/B) $(\propto 1/q)$. The effect of the sawteeth on confinement can be seen where the maximum incremental confinement time is reached for a value of $q \sim 4$ $(I_p/b \sim 1)$.

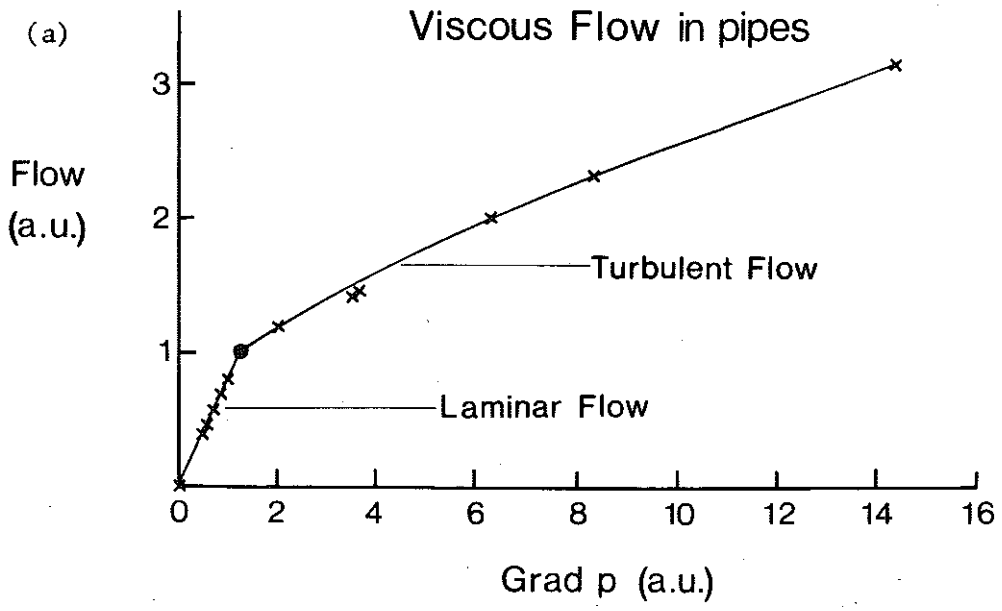

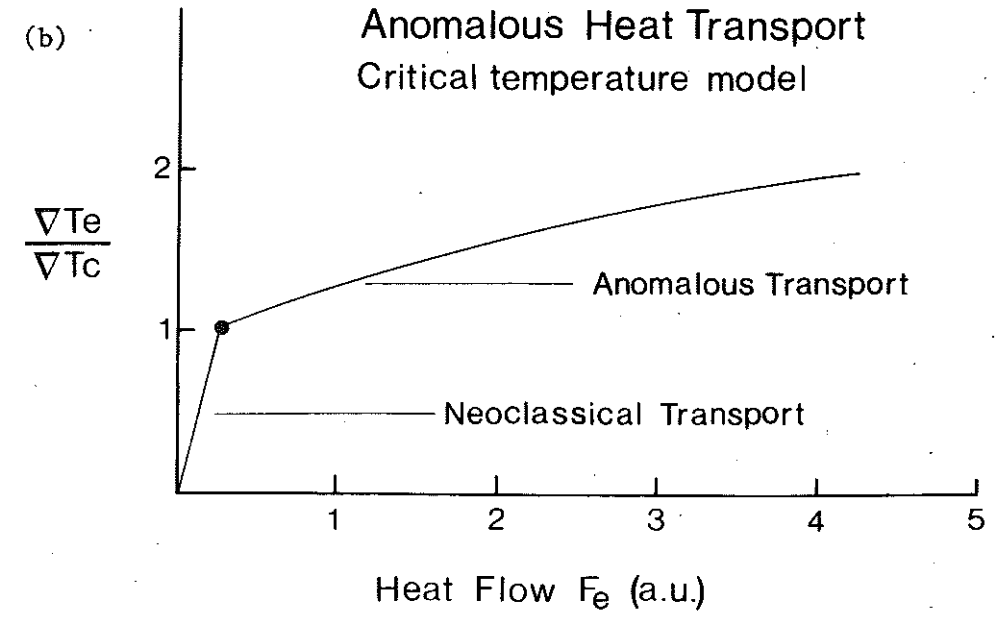

Fig. 13 (a) The experimental relationship governing the flow of a liquid through a long pipe is shown. When the Reynolds number R reaches the critical value R_c, extra resistance is added to the flow which increases with the value of the Reynolds number (curvature of the curve in the turbulent flow regime); (b) For given temperature, density, magnetic field etc., the dependence of the heat flow with electron temperature gradient in the critical temperature model shows the same behaviour: when ∇T *reaches* ∇T_c anomalous transport appears which increases the heat flow. This anomalous transport also varies non-linearly with the ratio ($\nabla T_e / \nabla T_c$).

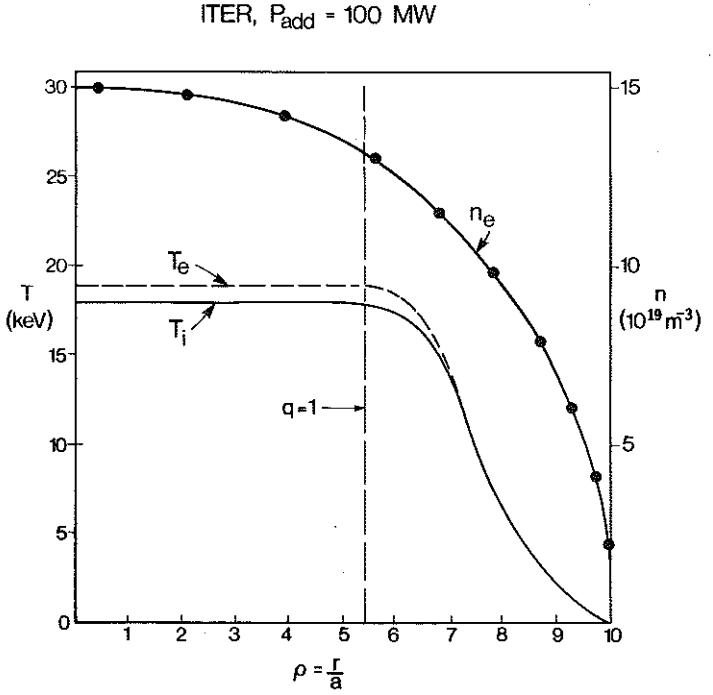

Fig. 14 Critical temperature model simulation of ITER with 300MW of additional power. Ignition is not reached mainly due to the effect of sawteeth. The temperature has been flattened inside the $q=1$ region.

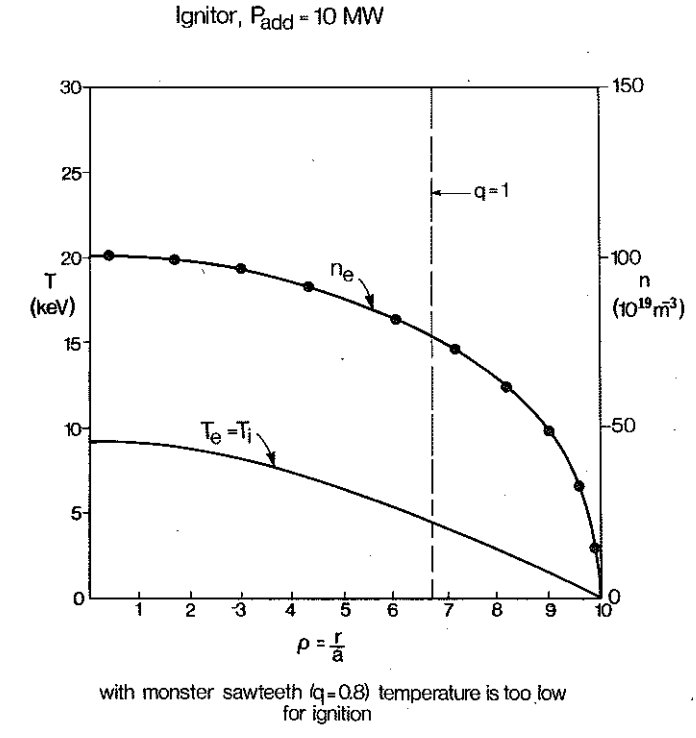

Fig. 15 Critical temperature model simulation of IGNITOR, with additional power of 10MW. The temperature has been allowed to peak inside the $q=1$, simulating a monster sawtooth with q on axis of 0.8. Ignition is not reached as the mean temperature is too low; Bremsstrahlung and impurity radiation play an important role ($Z_{eff}=2$).

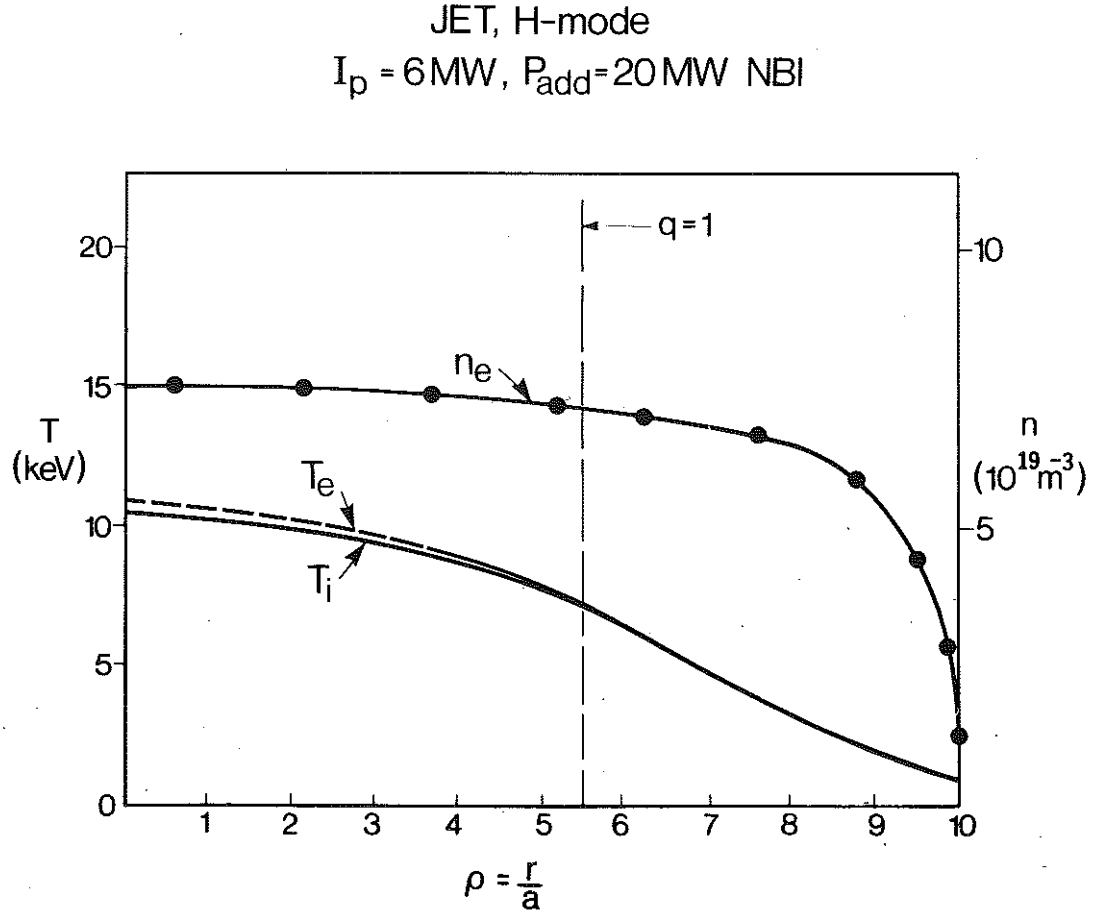

Fig. 16 JET H-modes are fully simulated if the experimental density profile is taken with a pedestal of 1–2 keV at the separatrix. The simulation is made for an H-mode at 6 MA with 20 MW of neutral beam power.

JIT at full Ignition, I_p = 20MA

(a)

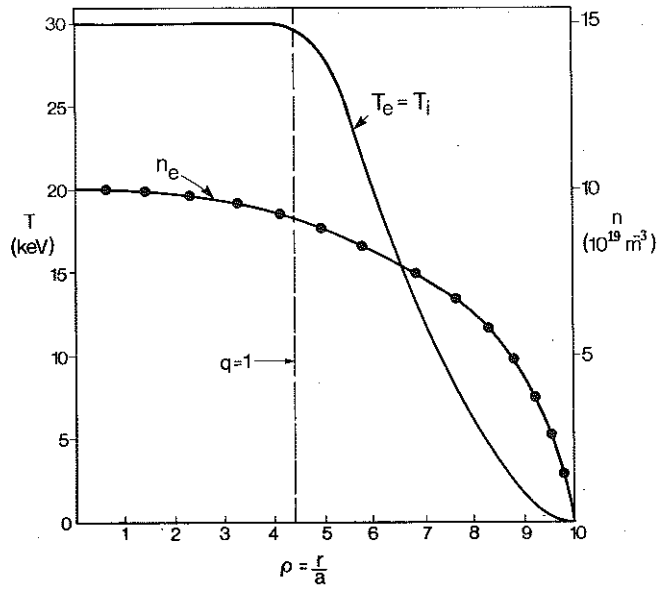

The sawteeth flatten the temperature inside q=1
P_F = 2.5 GW, g= 3 (β limit), V=0.07 Volt per turn

JIT ohmic + α heating, I_p = 30 MA

(b)

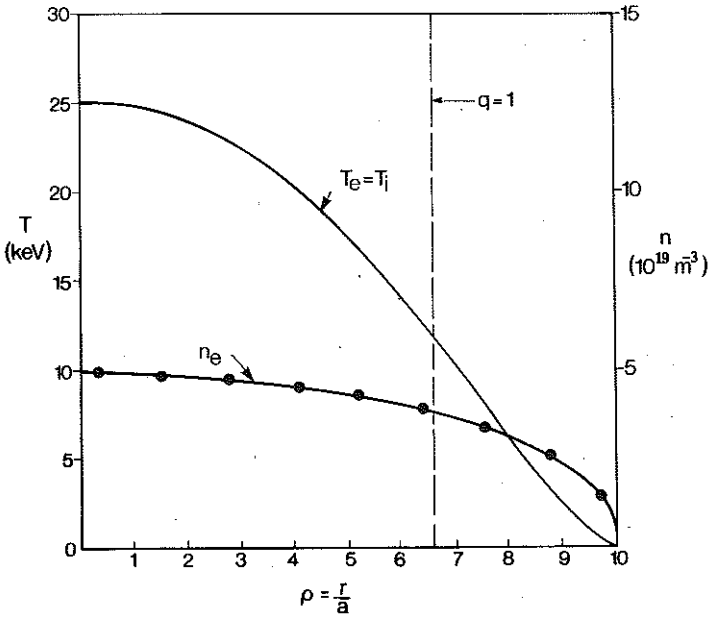

Ignition is reached with the help of monster sawteeth (q=0.8)

Fig. 17 (a) Critical temperature simulation of JIT. Full ignition is obtained on JIT even with complete flattening of the temperature inside the $q=1$ region at 20MA. The β limit ($g=3.6$) is almost reached; (b) At 30MA with a monster sawtooth, ignition is obtained without additional heating at a lower density.

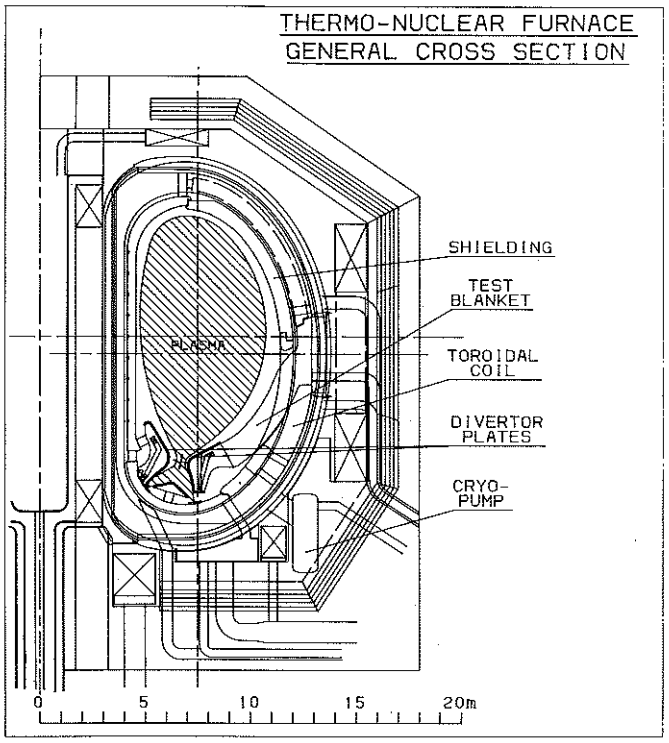

Fig. 18 Cross-section of a thermonuclear furnace (JIT) with a plasma capability of 30MA.

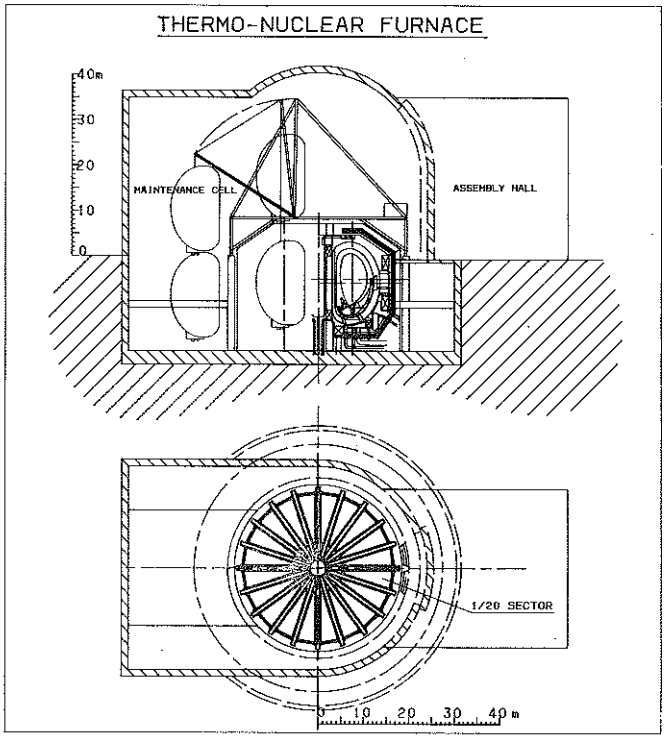

Fig. 19 Overall view of the thermonuclear furnace and the main building including the remote handling facilities and the external shielding.

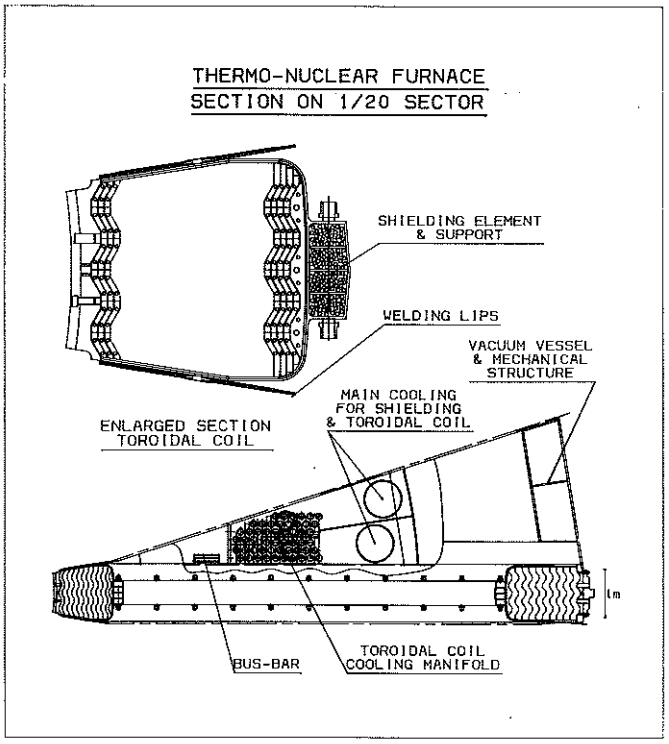

Fig. 20 Section of a sector of JIT conceived as an integrated element including the toroidal coil, the vacuum vessel, and the mechanical structure. Toroidal field coils are shown.

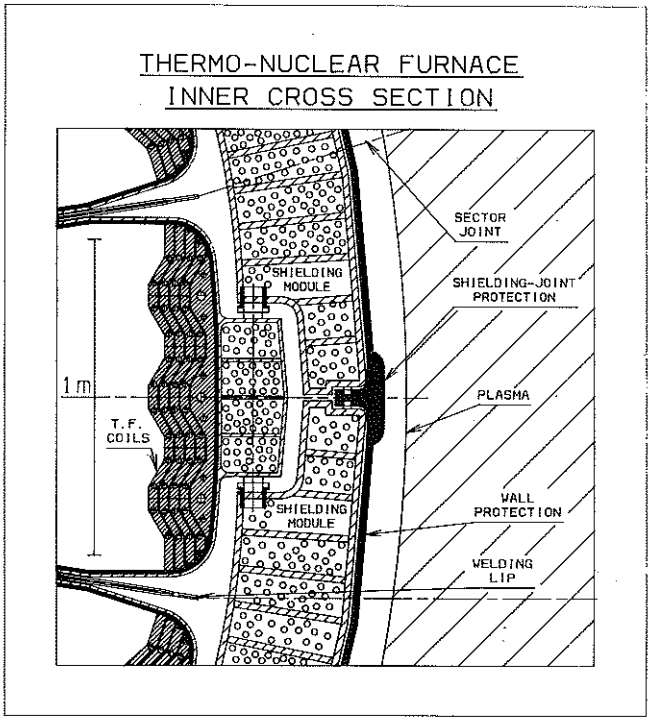

Fig. 21 The concept of the inner wall blanket supported by toroidal field coils and protected by carbon tiles.

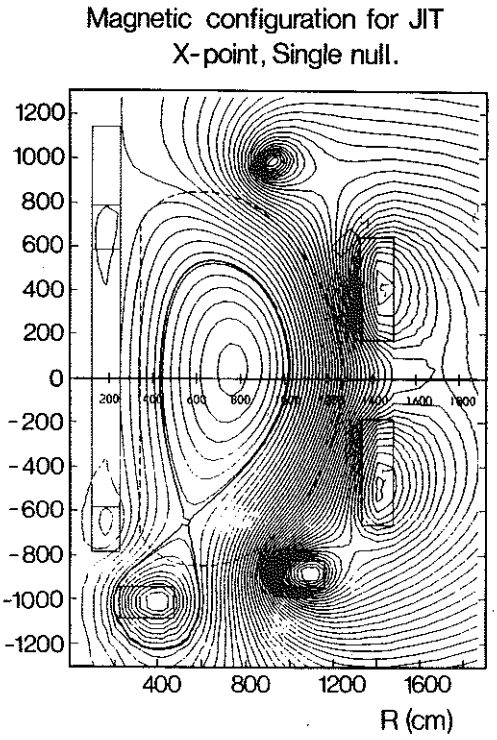

Fig. 22 Typical magnetic configuration calculated for JIT with a single X-point.

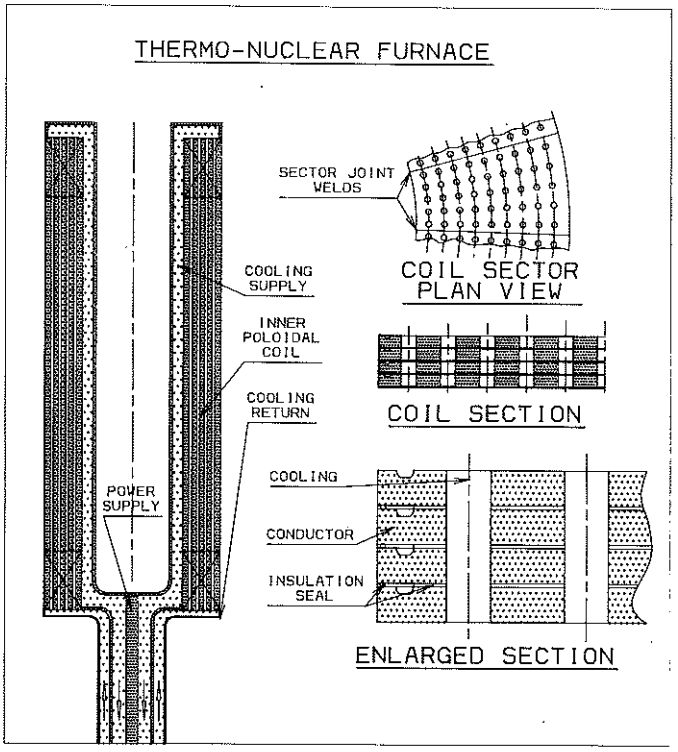

Fig. 23 The internal poloidal field coil, conceived as a Bitter coil with detail of the cooling and insulation.

(a)

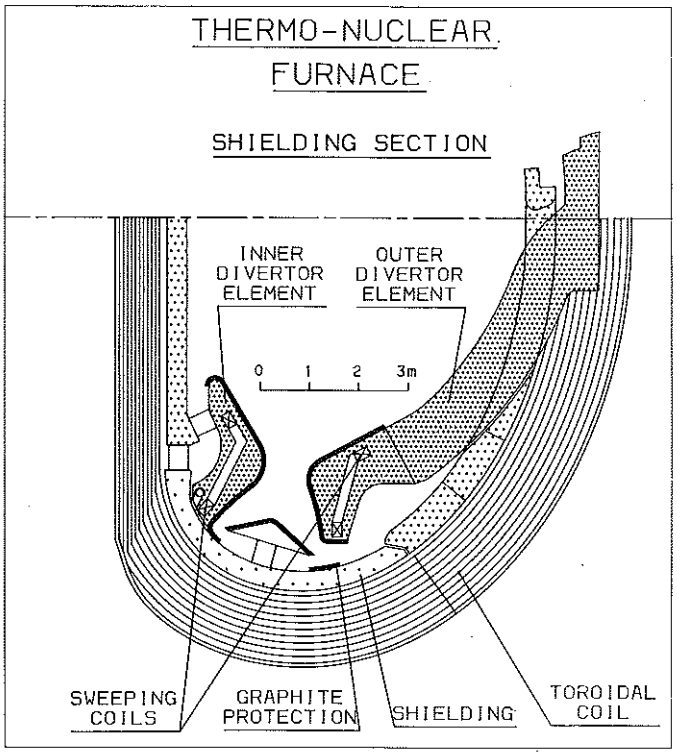

(b)

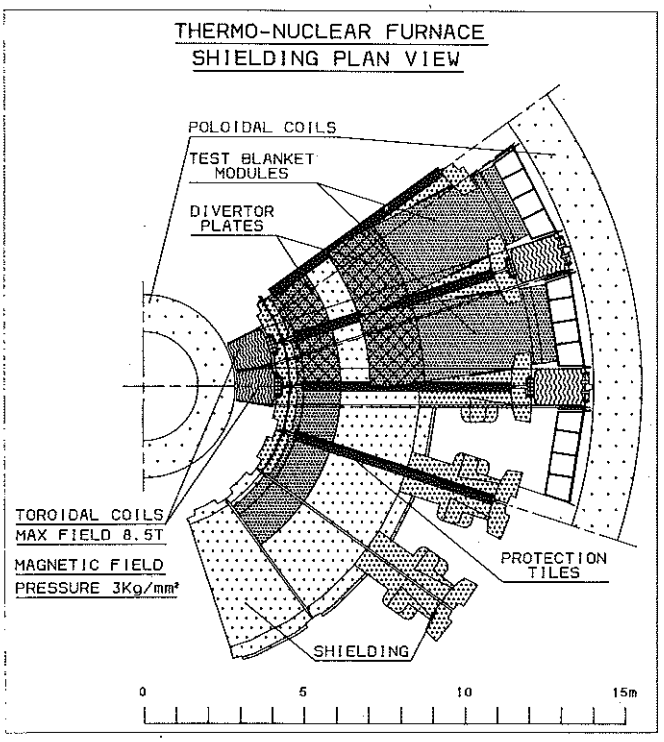

Fig. 24 (a) Sectional and (b) plan view of internal layout of JIT shielding, divertor element and test blanket which can be dismantled remotely through the main ports.

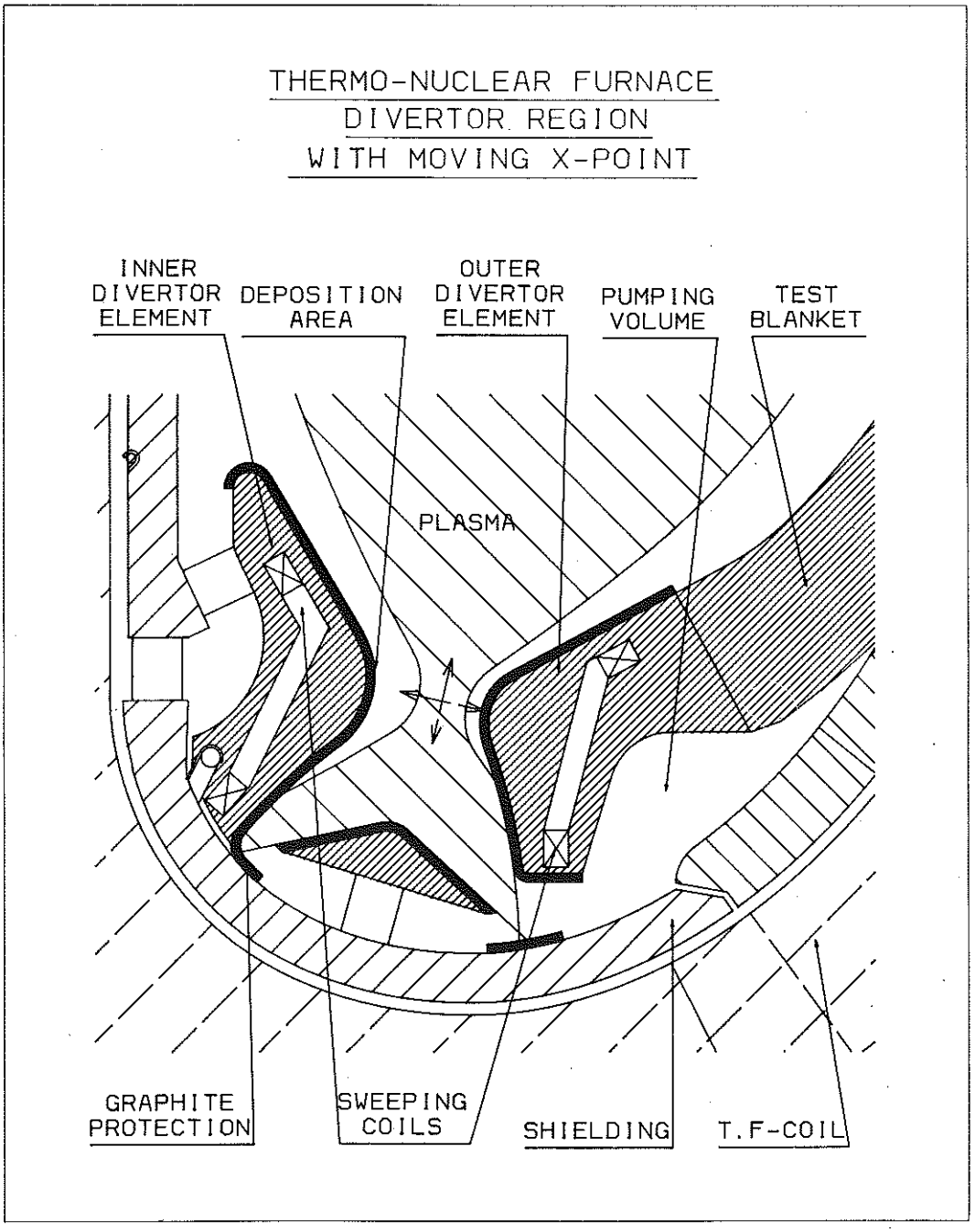

Fig. 25 Divertor region of JIT showing a set of saddle coils which allow sweeping of the thermal load on the divertor plates covered with graphite. Pumping is carried out through a slot at the base of the divertor.